MBE GROWTH AND INSTRUMENTATION

Sriteja Tarigopula

Thesis Prepared for the Degree of

MASTER OF SCIENCE

UNIVERSITY OF NORTH TEXAS

May 2006

APPROVED:

Shuping Wang, Major Professor
Terry Golding, Committee Member
Keith Jamison, Committee Member
Vijay Vaidyanathan, Committee Member and
Departmental Coordinator of Electronics
Engineering Technology
Albert B. Grubbs Jr., Committee Member and
Chair of Department of Engineering
Technology
Oscar Garcia, Dean of the College of Engineering
Sandra L. Terrell, Dean of the Robert B. Toulouse
School of Graduate Studies

Tarigopula, Sriteja, *MBE Growth and Instrumentation*, Master of Science (Engineering Technology), May 2006, 79 pp., 5 tables, 69 figures, references, 25 titles.

This thesis mainly aims at application of principles of engineering technology in the field of molecular beam epitaxy (MBE). MBE is a versatile technique for growing epitaxial thin films of semiconductors and metals by impinging molecular beams of atoms onto a heated substrate under ultra-high vacuum (UHV) conditions. Here, a LabVIEW® (laboratory virtual instrument engineering workbench) software[*] program is developed that would form the basis of a real-time control system that would transform MBE into a true-production technology. Growth conditions can be monitored in real-time with the help of reflection high energy electron diffraction (RHEED) technique. The period of one RHEED oscillation corresponds exactly to the growth of one monolayer of atoms of the semiconductor material. The PCI-1409 frame grabber card supplied by National Instruments is used in conjunction with the LabVIEW software to capture the RHEED images and capture the intensity of RHEED oscillations. The intensity values are written to a text file and plotted in the form of a graph. A fast Fourier transform of these oscillations gives the growth rate of the epi-wafer being grown. All the data being captured by the LabVIEW program can be saved to file forming a growth pedigree for future use. Unattended automation can be achieved by designing a control system that monitors the growth in real-time and compares it with the data recorded from the LabVIEW program from the previous growth and adjusts the growth parameters automatically thereby growing accurate device structures.

[*]National Instruments Corporation, http://www.ni.com/legal/termsofuse/unitedstates/us/

Copyright 2006

by

Sriteja Tarigopula

ACKNOWLEDGEMENTS

I thank my major professor Dr. Shuping Wang for her time, encouragement, attention to detail, and excellent guidance that have been necessary for this thesis.

I express my gratitude and thanks to my professor, supervisor and committee member Dr. Terry Golding for his support, confidence, encouragement and guidance throughout my graduate program and in completing this thesis.

I thank my committee member Dr. Vijay Vaidyanathan for his valuable suggestions, support and friendly guidance.

I thank the Dr. Albert B. Grubbs, Chair of Engineering Technology Department, University of North Texas, for his support and encouragement all along my graduate studies.

I express my gratitude to my Industrial representative Mr. Keith Jamison for his time and support.

I dedicate my thesis to my parents Mr. Sripathi Tarigopula and Mrs. Nagapushpavathy Tarigopula. I also like to thank my sister Srivamsi Tarigopula and my brother Srinath Chowdary Tarigopula for their support and encouragement.

I would also like to thank my friends Arun Yelimeli, Dr. Brian Gorman, Ryan Cottier, Dr.Fatima Amir, Sheetal Liddar, Rekha Vemuri for their help, suggestions and their valuable time.

TABLE OF CONTENTS

Page

ACKNOWLEDGMENTS iii

LIST OF TABLES v

LIST OF FIGURES vi

Chapters

I. INTRODUCTION 1
MBE as a Production Technology
Statement of Need
Purpose of Study
Hypothesis

II. REVIEW OF LITERATURE 12
Molecular Beam Epitaxy Background
Interference Phenomenon in Light Waves
Electron Diffraction
Reflection High Energy Electron Diffraction

III. METHODOLOGY/ACQUISITION OF DATA 25
Preparing the III/V Chamber of Growth
Experimental Setup for LabVIEW®

IV. RESULTS AND DISCUSSION 53
Limitations

V. CONCLUSIONS 73

VI. FUTURE WORK 76

REFERENCES 78

LIST OF TABLES

Page

1. RHEED data from LabVIEW® program.. 56

2. Reconstruction of RHEED oscillations in ORIGIN program.. 57

3. Reconstruction of RHEED oscillations in ORIGIN for Dr.Gossmann's program for sample-1 57

4. Reconstruction of RHEED oscillations in ORIGIN program for LabVIEW® for sample-2 62

5. Reconstruction of RHEED oscillations in ORIGIN for Dr.Gossmann's program for sample-2 62

LIST OF FIGURES

Page

1. Schematic illustration of basic evaporation process for molecular beam epitaxy for intentionally doped GaAs Al_xGa_{1-x} [11] ... 3

2. RHEED Gun setup for MBE growth [11] ... 4

3. Block diagram of the control until that can be designed depending on the RHEED oscillations ... 6

4. Schematic cross section of an advanced three- chamber UHV system designed for MBE growth and detailed surface studies [16] ... 14

5. Constructive interference and destructive interference in waves [16] ... 15

6. Formation of bright and dark streaks of light due to constructive and destructive interference of light waves [16] ... 16

7. Crystal translational vectors a,b,c depicting the crystal axis in x,y,z directions [17] ... 18

8. The above figure shows crystal lattice in a 2-dimensional space. The atomic arrangement in the crystal looks exactly the same to an observer at r' and r, provided that the vector T which connects r' and r may be expressed as an integral multiple of vectors a and b [17]. ... 18

9. Space lattice [17] ... 19

10. Basis, containing two different ions [17] ... 19

11. Crystal structure [17] ... 19

12. Ewald's sphere for the construction of diffraction pattern in reciprocal lattice space [17] ... 23

13. Varian 360, III/V MBE growth chamber at UNT ... 26

14. Group IV MBE system at UNT ... 26

15. Flow diagram to represent the experimental procedure of the III/V MBE ... 27

16. Vacuum pumps on the III/V MBE system ... 28

17. Ion pump and cryo-pump on the III/V MBE system ... 29

18. Load-lock chamber of the III/V MBE system ... 31

19. View port of the load-lock chamber showing the molybdenum blocks and samples ... 32

20. Preparation chamber of the III/V MBE system 33

21. Top view of a typical standard MBE system growth chamber [20] 34

22. Growth chamber of III/V MBE system 36

23. Screen shot of the SpecView program 36

24. Furnace control unit housing rack 37

25. RHEED control Equipment housing rack 38

26. PCI-1409 frame grabber card supplied by National Instruments [23] 39

27. Experimental setup to capture RHEED images of the III/V MBE chamber using the LabVIEW® code 40

28. Flow diagram depicting the functioning of the LabVIEW® code 41

29. Front panel showing the various controls for the program 44

30. Front panel showing the Waveform Chart 45

31. Front panel having the ERROR INDICATORS at various stages of the program 46

32. Sequence 0, used to select a point on the image at which the measurements will be taken 47

33. Sequence 1, configuring IMAQ buffers for acquisition 48

34. In Sequence 2, a decision is made whether to start the acquisition or to wait further 49

35. Sequence 3, displays an image and measures the intensity on the image 50

36. Sequence 3 also stops acquisition and writes the data to file 51

37. Sequence 4, writes images to file 52

38. Sequence 5, closes the acquisition and releases IMAQ buffers in system memory 52

39. RHEED oscillations for sample-1 and sample-2 recorded usingLabVIEW® program 54

40. RHEED image before growing Fe for sample-1 54

41. RHEED image for sample-1 during the growth 54

42. RHEED image for sample-1 after finishing Fe deposition 55

43. Reconstruction of RHEED oscillations forLabVIEW® using ORIGIN 58
44. Reconstruction of RHEED oscillations for Dr.Gossmann's program using ORIGIN.... 58
45. FFT forLabVIEW® for sample-1 59
46. FFT for Dr.Gossmann's program for sample-1 59
47. RHEED reconstruction for sample-2 forLabVIEW® program 60
48. RHEED reconstruction for sample-2 for Dr.Gossmann's program 61
49. RHEED image before deposition of Fe on sample-2 61
50. RHEED image during deposition of Fe on sample-2 63
51. RHEED image after depositing of Fe on sample-2 63
52. FFT for LabVIEW® program for sample-2 64
53. FFT for Dr.Gossmann's program for sample-2 64
54. RHEED intensity recording for sample-3 65
55. RHEED image during initial deposition of Si 66
56. RHEED image after depositing Si for 8 minutes 67
57. RHEED image when the Fe source is opened 67
58. RHEED image after depositing Fe for 15 minutes 68
59. RHEED image after Ge source is opened 68
60. RHEED image after depositing Ge for 2 minutes 69
61. RHEED image at the end of depositing Ge 69
62. Growth pattern reconstructed using ORIGIN software 70
63. FFT of oscillations for Si growth 71
64. FFT oscillations for Fe Growth 71
65. FFT oscillations for Ge 72
66. MBE system with a feedback control system associated with it. 76

CHAPTER 1

INTRODUCTION

World's engineers provide service to a wide range of fields ranging from electronics, electrical, mechanical, civil, construction to physics, chemistry, transportation, efficient energy use, new materials, fabrication, new products and manufacturing processes. Engineering Technology focuses on technological systems and processes with specific industrial applications. Electronics engineering technology covers hardware and software interfacing, data acquisition and analysis, computer-aided software engineering, real-time control systems, digital signal processing and so on. This thesis mainly aims at taking a step towards application of engineering technology in the field of physics.

Semiconductor structures constitute the building blocks of several electronic and photonic devices such as such as field effect transistors (FET) [1], hetrojunction bipolar transistors (HBTs) [2], metal semiconductor field effect transistor (MSFET) [3], high electron mobility transistors (HEMT) [4], high speed integrated circuits on a single wafer [5], laser diodes [6], photo detectors [7], light emitting diodes [8], vertical cavity surface emitting laser (VCSEL) [9]. These devices are used in such applications as fiber-optics, cellular phones, satellites, radar systems, display devices, microwave devices, radio frequency (RF) devices, Bluetooth wireless technology, flat panel displays, satellite radio, global positioning system (GPS), wireless local area network (LAN) [10]. The ever growing demand of high performance semiconductor devices calls for a need of controlled and precise growth of the semiconductor compounds to achieve the targeted device properties. Consider for example a VCSEL. In this device the laser is emitted vertical to the surface of the device. The efficiency of the laser depends of the surface roughness of the Bragg reflecting mirrors that have very small dimensions (~50nm) and are stacked one

over the other. Precise growth of these layers needs very controlled and stringent growth mechanism.

The choice of semiconductors for synthesizing particular device application is guided by the specific electrical or optical design requirements, coupled with an ability to grow the required stack of semiconductor layers epitaxially. Epitaxy is the process of depositing, or growing, atomically thin crystal layers of typically dissimilar elemental materials onto a substrate to produce a compound semiconductor. Each crystal layer is known as an epilayer. After the epilayers are grown on a substrate, it is known as an epiwafer. A novel and the most popular means to achieve these requirements is to use the molecular beam epitaxy (MBE) growth process. MBE is a versatile technique for growing epitaxial thin films of semiconductors and metals by impinging molecular beams of atoms onto a heated substrate under ultra-high vacuum (UHV) conditions. The basic evaporation process during in the MBE chamber present in UNT is schematically depicted in Figure 1. The illustration shows the heated substrate. The molecular beams (flux) reacting on the substrate crystal are generated by thermal evaporation of the constituent elements or their compounds contained in accurately temperature-controlled effusion cells. These cells are arranged such that the central portion of their flux distribution intersects the substrate at an orifice-substrate distance ranging from 60 to 140 mm in various MBE systems [11]. Each source is provided a shutter that can be controlled mechanically or pneumatically. Operation of these shutters permits rapid changing of the beam species in order to alter abruptly the composition and/or doping of growing film normal to the surface with a slow growth rate of up to 0.1-2.0μm/hr. As a consequence, abrupt material interfaces can be achieved, since any significant bulk diffusion is eliminated at the specific low growth temperature of MBE. In

addition, mechanical masks may be inserted into the paths of the beam fluxes to create any desired device geometry.

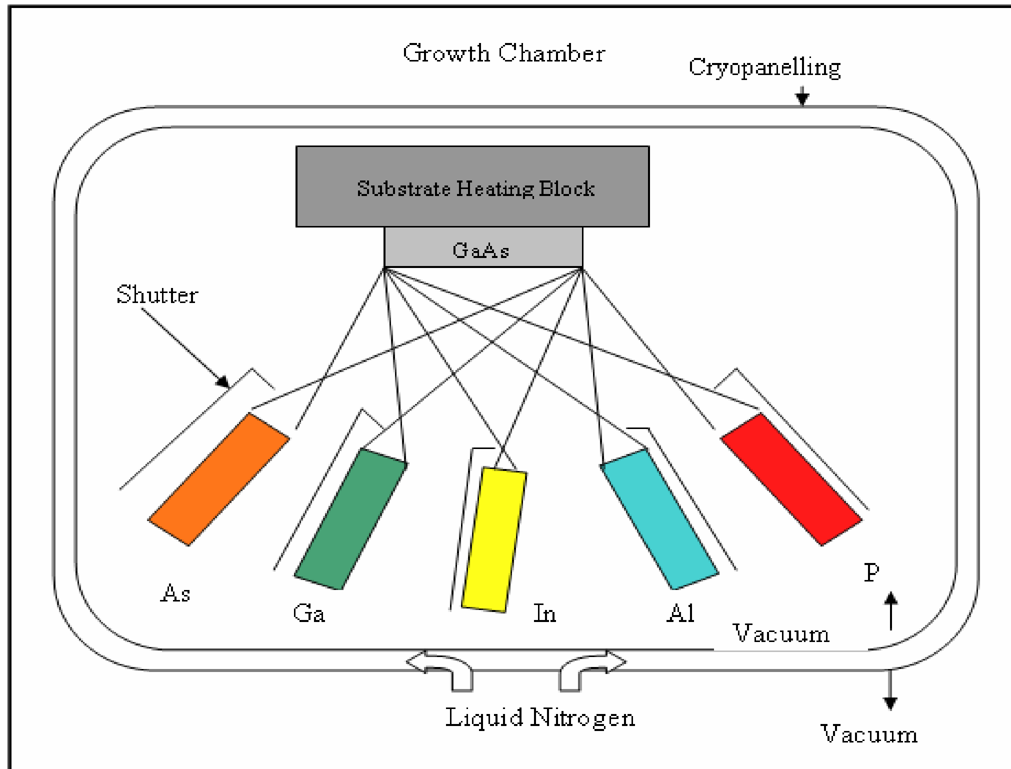

Figure 1. Schematic illustration of basic evaporation process for molecular beam epitaxy for III/IV MBE chamber present in University of North Texas (UNT).

MBE allows growth of crystalline layer combinations with accurate dimensional control down to the atomic level. This precision would not be possible without adequate accurate characterization techniques. One of the most useful tools for *in situ* monitoring of the crystal growth is the reflection high-energy electron diffraction (RHEED) system. RHEED provides resolution on the atomic scale while at the same time being fully compatible with the crystal growth process. The layout of a typical RHEED system is shown in Figure 2. A typical RHEED measurement system consists of an electron gun, a phosphor screen and image processing hardware and software. The RHEED gun emits ~10KeV electrons which impinge the semiconductor surface at a shallow angle (~0.5-2°) [11]. The incident electrons diffract from the

surface of the sample wafer and strike a phosphor screen forming a pattern of dark and bright lines, which is indicative of the surface crystal structure. A camera monitors the screen and can record instantaneous pictures or measure the intensity of the image at a given pixel as a function of time. The intensity of the RHEED image keeps changing from time to time or in other words the intensity keeps oscillating. It has been well established that the period of these oscillations corresponds exactly to the growth of one monolayer of atoms of the semiconductor material during the growth [12]. RHEED is therefore used to calibrate growth rates, observe removal of oxides from the surface, calibrate the substrate temperature and monitor the arrangement of the surface atoms and to give a feedback on surface morphology during growth.

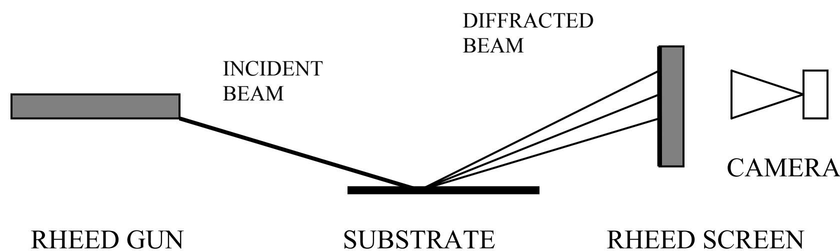

Figure 2. RHEED Gun setup for MBE growth. Adapted from [11].

MBE as a Production Technology

MBE has gone through a lot of development and refinement over the past two decades and has transformed itself to near production-ready technology. Commercial MBE vendors have made a great amount of progress in terms of producing clean wafers and source cells with accurate dimensions. For advanced epi-based structures such as HEMTs and HBTs, MBE is capable of preparing these extremely complex structures with atomic layer precision. However, important concerns in mass production of these materials are reproducibility from run to run, over period of times and from systems to systems. Frequent system calibration runs and test runs

still have to be prepared routinely. These non-productive runs increase average cost and reduce growth yield. Moreover, processing specifications of many devices are tightened because Stricter tolerance of certain critical parameters can significantly impact the cost of producing high-performance, low cost modules and circuits. This calls for automating the MBE growth process to improve wafer to wafer processing repeatability, reduce run-time by eliminating error prone process to produce devices on a large scale without compromising on the quality of the device structures grown.

Unattended automation can be achieved by designing a control system that monitors the growth in real-time and compares it with the data available from the previous growth. The difference between the real-time data and ideal data can be calculated and feedback to the control system and the growth parameters can be adjusted in real-time, thereby achieving accurate device structures. The variables that strongly effect the layer growth are the substrate temperature and flux emitting from the individual source materials. In the MBE reactor, it is not possible to rapidly change the diffusion (by controlling surface temperature) over the time period of typical 5-10 monolayer growth because of the slow thermal dynamics of the substrate. Hence, substrate temperature is useful as a "run-to-run" control variable. Flux on the other hand can be rapidly changed by adjusting the effusion cell shutters, and more slowly changed by controlling the cell temperature. Hence, flux is the effective control variable. A change in flux will effect the deposition time to achieve a desired coverage, i.e., decreasing flux increases the deposition time to reach a coverage goal and vice versa.

Growth conditions can be monitored in real-time with the help of RHEED data, since the period of one RHEED oscillation corresponds exactly to the growth of one monolayer of atoms of the semiconductor material [12]. These RHEED oscillation patterns can be observed from

time to time and compared to previously available data of the same material being grown. If it is observed that a known growth pattern is not being followed then the growth conditions such as the temperature of the source cells and also control the movement of the shutters in front of the source cells can be altered. A schematic depiction of such a system is shown in Figure 3 . The wafers are grown in the MBE chamber, and the RHEED images are observed on the computer and the real-time data is compared against the already available data. If any changes are to be made in the growth conditions, the computer calculates these values and sends the signals to change the temperature of the source cells or the control the movement of the shutters in front of the source cells. In addition to this, the current data being captured can also be saved for future reference.

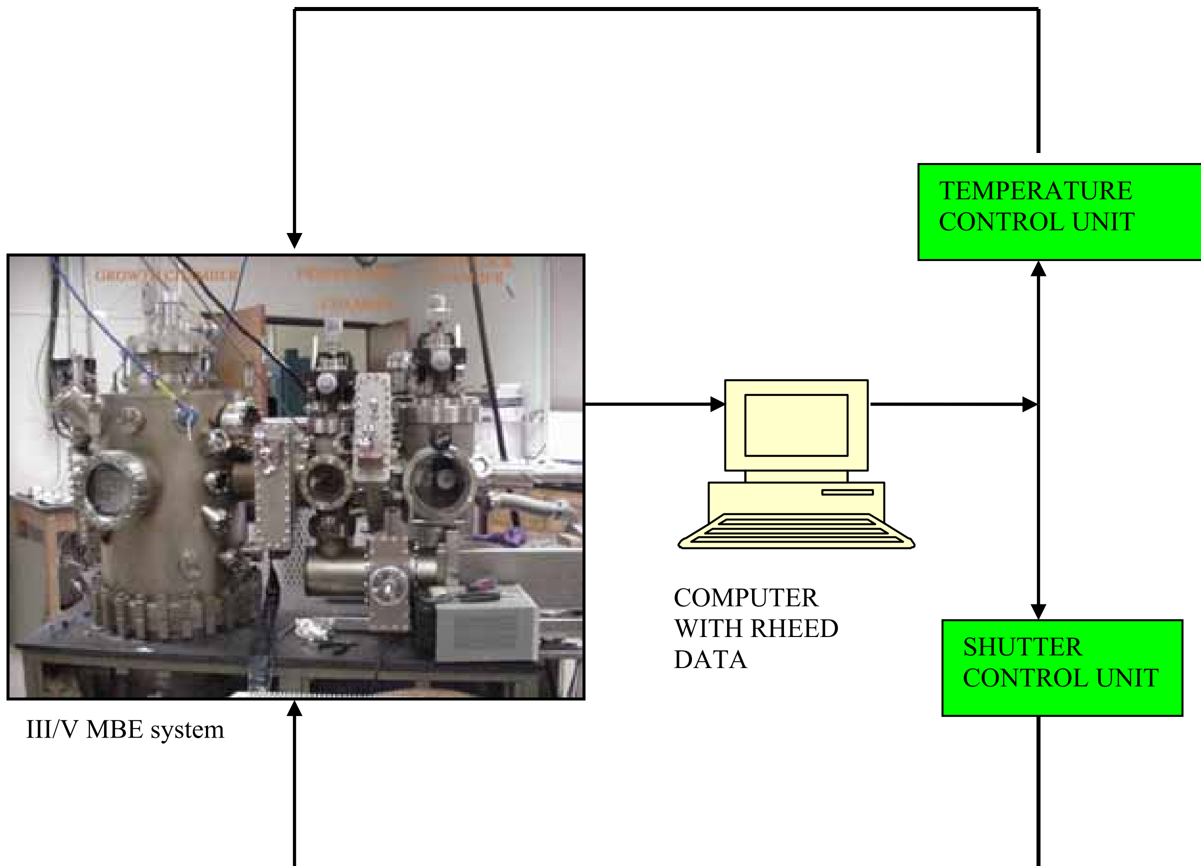

Figure 3. Block diagram of the control until that can be designed depending on the RHEED oscillations.

Statement of Need

RHEED oscillations can be monitored either manually or by using a software program. The software that was present in the III/VMBE lab to record the RHEED data is called the Video RHEED Intensity Measurement Program (RHEED program) [13]. With this system, the intensity of diffracted beams can be measured simultaneously. The RHEED program used a Panasonic™ CCD camera[*] (Model No: WV-BD400) to monitor the images continuously and take the intensity measurements using a video card. The intensity of the diffracted beams is also displayed in real time on the video monitor, enabling the user to monitor the growth in real time. After data acquisition is finished, the RHEED intensity oscillations are either scanned with a movable cursor to determine the period of the oscillations or analyzed using a fast Fourier transform (FFT) to give a growth rate.

The video intensity measurement board is not a "frame grabber". Instead, it breaks up the video screen into a matrix of 256*256 pixels with 256 gray levels per pixel. The intensity from a given pixel is read by sending the address of that pixel to the video digitizing board, waiting until the chosen pixel is digitized, and then reading the digitized intensity. The video digitizing board displays a bright point at the selected pixel location on the video monitor while the selected pixel is digitized.

At normal video camera line frequency (~15 KHz), the video digitizing board can digitize one data point with each horizontal line scan of the video camera. Therefore, the maximum data acquisition rate is one vertical line (having a maximum of 256 points) every 1/60th of a second. Because a normal video signal is composed of 2 interlaced 256 line scans, it is possible to record a vertical line of 512 points every 1/30th of a second. Data acquisition speed of the video digitizing board is optimized by using vertical data windows one pixel wide that do not overlap

[*] Matsushita Electric Industrial Co., Ltd., http://www.panasonic.com/pol_docs/copyright-prv.html

horizontally. Increasing the data window width reduces the data acquisition speed by the inverse of the window width. (Data acquisition speed = window width/60 seconds per point for non overlapping windows).

However, this program crashed and could not be restored. The company that supplied this software is closed, so a replacement could not be obtained. When the software was functional, the program did not have an option to record the images before, during and after the growth of the semiconductor material. It is important to save the RHEED images so that they can be used in future growths when similar materials are being grown. For example, if a sample material is grown in ideal conditions and gives accurate results, the RHEED images obtained during this growth cycle can be used to compare with the RHEED images that are obtained during mass production. If it is seen during a sample growth (during mass production) that the RHEED images differ from the ideal images already available then, necessary corrections can be made to the growth conditions.

Also, the data was recorded only in the form of a graph, it could not be written to a file like an EXCEL sheet so that it could be analyzed further for more accurate results. For example, if the data was being recorded every 0.03 seconds, and large number of oscillations are observed between 1.35 to 1.39 seconds. Then there is no way of zooming in and out of these oscillations in a given time range for in-depth study of these oscillations. And since the data cannot be written to an external file, it cannot be reproduced again for further analysis.

Also, if the recording of oscillations was stopped at a particular point of time, (like to alter the temperature of the sample being grown or the temperature of the source cell) new oscillations could not be appended to the existing file which makes it difficult to observe the

change in oscillations accurately when the temperature is varied. Each time a new file had to be opened to record the oscillations.

Also, the RHEED program used two different monitors to run the program, one to view the images (a video monitor) and one to display the oscillations (computer). The user did not have a choice to change or specify the rate at which the oscillations are recorded like every 0.05 seconds or 0.07 seconds. Also the RHEED program and the video card did not have the necessary software and hardware interface associated with it so that it can form the basis of a real-time control unit as shown in Figure 3.

Purpose of Study

The main purpose of the study is to develop a software program which would form the basis of *in situ* monitoring of MBE growth for the development of a production ready MBE.

TheLabVIEW® (laboratory virtual instrument engineering workbench) software[*] has the necessary software to overcome the limitations in the Video RHEED Intensity Measurement Program. The PCI-1409 frame grabber card also supplied by National Instruments is used in association with the LabVIEW® software to capture the RHEED images and calculate the intensity of the oscillations. The LabVIEW® program developed in the lab performs the following functions:

1. Measure the intensity at a particular point on the image through a Panasonic CCD camera and using a frame grabber card (PCI-1409) to read the intensity values. Plot the intensity values as Time vs. Amplitude graph.
2. Observe the RHEED images continuously on the same computer monitor that has the LabVIEW® code in it. The record the RHEED images before, during and at the end of the sample growth. Able to change the point of measurement on the image during the growth.

[*]National Instruments Corporation, http://www.ni.com/legal/termsofuse/unitedstates/us/

3. Write the recorded intensity and the time values to an EXCEL spreadsheet. While growing different samples the user should have a choice to append the data to an existing file or write data to a new file. The program has flexibility to record the intensity values at different time intervals such as 20ms, 50 ms or 30ms and so on as specified by the user.

4. User friendly interface, the end-user need not have a working knowledge of LabVIEW® to operate the program.

5. This program is portable. That is it does not depend on the MBE system that is being used to take the measurements. It can be used in conjunction with any MBE system that has RHEED in it.

Once the data is obtained the fast Fourier transformation (FFT) calculations will be made on the data to calculate the crystal growth rate. The research will also include operating the electronics associated with the III/V MBE system to get a real world experience of the semi-conductor industrial technology. Since there is a need to validate the results obtained using the new LabVIEW® code, these results are compared to an existing RHEED program present on the group IV MBE system in the lab. The GROUP IV MBE uses a program developed by Dr. Hans Gossmann to record the RHEED oscillations. This program is similar to the Video RHEED Intensity Measurement Program with a single exception that the data can be written to a text file (.txt) file. The LabVIEW® program has been able to achieve similar results as in Dr.Gossmann's program. The program is now working and it can be further expanded to have a real-time control system shown in Figure 3.

Hypotheses

Null Hypothesis: A working LabVIEW® code cannot be written as an alternative to the Video RHEED Intensity Measurement Program, to monitor the growth of semiconductor materials grown using the III/V MBE system.

Alternate Hypothesis: A working LabVIEW® program can be created as an alternative to the Video RHEED Intensity Measurement Program, to monitor the growth of semiconductor materials grown using the III/V MBE system.

CHAPTER II

REVIEW OF LITERATURE

Molecular Beam Epitaxy Background

The original ideas for molecular beam epitaxy (MBE) of III-V compound semiconductors was first proposed by Gunther in 1958 [14], it was not until 10 years later that epitaxy of mono-cyrstalline GaAs layers was achieved [15] using high improved vacuum conditions. MBE is a form of evaporation. It distinguishes itself from other evaporative crystal growth methods by employing a design that allows high quality epitaxial layers, with excellent carrier transport and optical properties to be prepared. The pursuit of higher vacuum conditions, by incorporation of a liquid-nitrogen-cooled shroud surrounding the evaporation sources and the use of ultra high vacuum pumps, achieved a pressure of about 10^{-9} torr in the early 1970s. It was the *in-situ* evaluation of crystal growth condition by reflection high-energy electron diffraction (RHEED) that led to the understanding of substrate cleaning, a proper epitaxial growth temperature and deposition rate.

The guidelines for achieving stoichiometric compounds by MBE have been found [15] in the surface chemical dependence of the sticking coefficient, *S*, of various species. *S* is defined as the fraction of total impinging atoms or molecules that sticks to the surface and is incorporated in the film. Generally, for III/V compounds only that amount of the group V element adheres to the growing surface, which collides with excess group III atoms on the surface and reacts to form the III-V crystal. As a result, one group V atom sticks for each group III atom, and epitaxial growth on the III-V substrate occurs [16].

During the growth process temperatures of the individual effusion cells control the intensities of beams incident on the heated substrate crystal. For typical growth rates of ~1μm/hr,

the fluxes required on the growing surfaces are approximately, 10^{14}-10^{15} atoms/ cm^{2}s for group III elements, 10^{15}-10^{16} atoms/ cm^{2}s for group V elements and 10^7-10^{12} atoms/cm^2 s for dopants [15]. Continuous changes in the chemical composition of the growing film are achieved by programmed variation of the cell temperatures. As mentioned earlier, abrupt changes are obtained by using mechanical shutters interposed between the cell orifice and substrate. The group III element beam is always atomic, while the beam of the group V element can be either diatomic when generated by incongruent evaporation of the III-V compound itself or tetratomic when generated from elemental source.

The slow growth rate during MBE coupled with obvious stringent demand for low unintentional impurity levels incorporated in the deposited material require a clean UHV environment in the growth chamber. Thus, the equipment for MBE is basically a stainless steel UHV system with a background pressure below 10^{-10} Torr pumped by standard ion pumps or by suitably trapped diffusion or turbomolecular pumps, respectively. Additional liquid nitrogen (LN_2) cryopanels assure that the partial pressures of gases with high sticking coefficient. (E.g. OH-containing species), are kept even below 10^{-14} Torr in the vicinity of the growing crystal [15]. In practice, during deposition, the total pressure in the reaction chamber rises above 10^{-9} Torr because of the scattered beam species. However, the UHV condition is always maintained with respect to impurity species.

A complete multichamber system designed for growing and extensively characterizing surfaces and multilayer epitaxial films is schematically depicted in Figure 4. The system utilizes three separate vacuum chambers connected via large diameter channels and isolation valves in a linear or angular configuration. The integral self-contained system essential for the crystal growth consists of the growth chamber and the load lock chamber/sample introduction chamber.

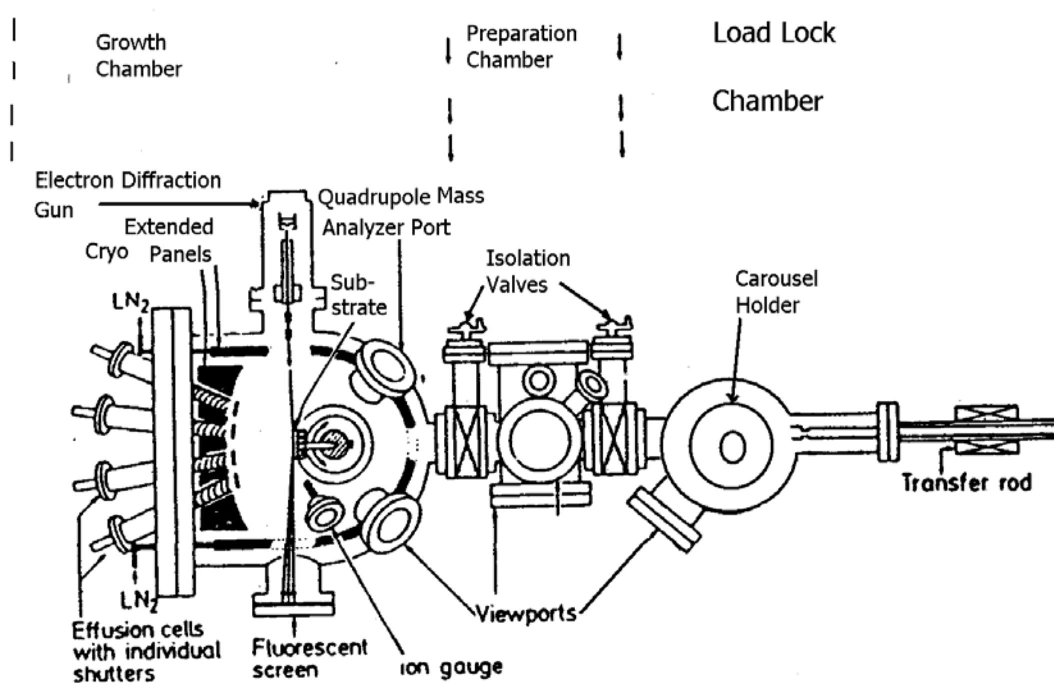

Figure 4. Schematic cross section of an advanced three- chamber UHV system designed for MBE growth and detailed surface studies. [15]. Reproduced with permission from Springer Science and Business Media.

One of MBE's big advantages is the fact that hazardous chemicals are usually handled in solid form and contained within the vacuum vessel, reducing the cost of external safety measures. The characteristic features of MBE are as described as follows [15]:

1. The slow growth rate of 0.1-2.0μm/hr that permits very precise control of layer thickness in the submicron range.
2. Reduced growth temperature, e.g., 500-600°C for GaAs.
3. Specific non-equilibrium growth mechanism that is responsible for progressive smoothing of the surface for most substrate orientations.
4. The ability to abruptly cease or initiate molecular beams that produces hyperabrupt material interfaces and dopant profiles
5. Facility for *in situ* analysis to assure that desired surface and reaction conditions are reached before commencement of growth and are maintained during crystal growth.

Therefore, the study of MBE plays an important role in the development of high performance semiconductors used for several electronic and photonic devices.

Interference Phenomenon in Light Waves

Interference is the superposition (overlapping) of two or more waves (having same frequency) resulting in a new wave pattern [16]. Consider two waves shown in Figure 5. When two waves superimpose, the resulting waveform depends on the frequency, (or wavelength) amplitude and relative phase of the two waves. If the two waves have the same amplitude A and wavelength the resultant waveform will have amplitude between 0 and 2A depending on whether the two waves are in phase or out of phase.

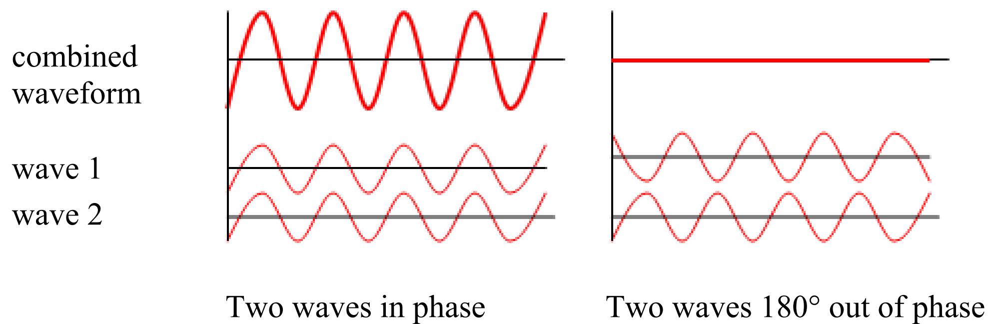

Figure 5. Constructive interference and destructive interference in waves. Adapted from [16].

Consider two waves that are in phase, with amplitudes A1 and A2. Their troughs and peaks line up and the resultant wave will have amplitude $A = A1 + A2$. This is known as constructive interference. If the two wave's are 180° out of phase, then one wave's hump will coincide with another wave's trough and so will tend to cancel out, resulting in destructive interference. The resultant amplitude is $A = |A1 - A2|$. If $A1 = A2$ the resultant amplitude will be

zero. Thomas Young demonstrated this phenomenon in light waves through his popular experiment known as the Young's experiment. Consider two coherent light sources spaced closely at two narrow slits, shown in

Figure **6**. In such an arrangement, the light waves emerging from the slits are in phase and this leads to a pattern of bright and dark bands on the screen called as interference fringes when a screen is placed in the path of these waves. Whenever constructive interference occurs between the two light sources a bright fringe is observed on the screen, shown in

Figure **6**. When destructive interference occurs between the two light sources a dark fringe is observed on the screen. This leads to a pattern of bright and dark fringes on the screen. This experiment can also be performed on a beam of electrons and atoms showing similar interference patterns.

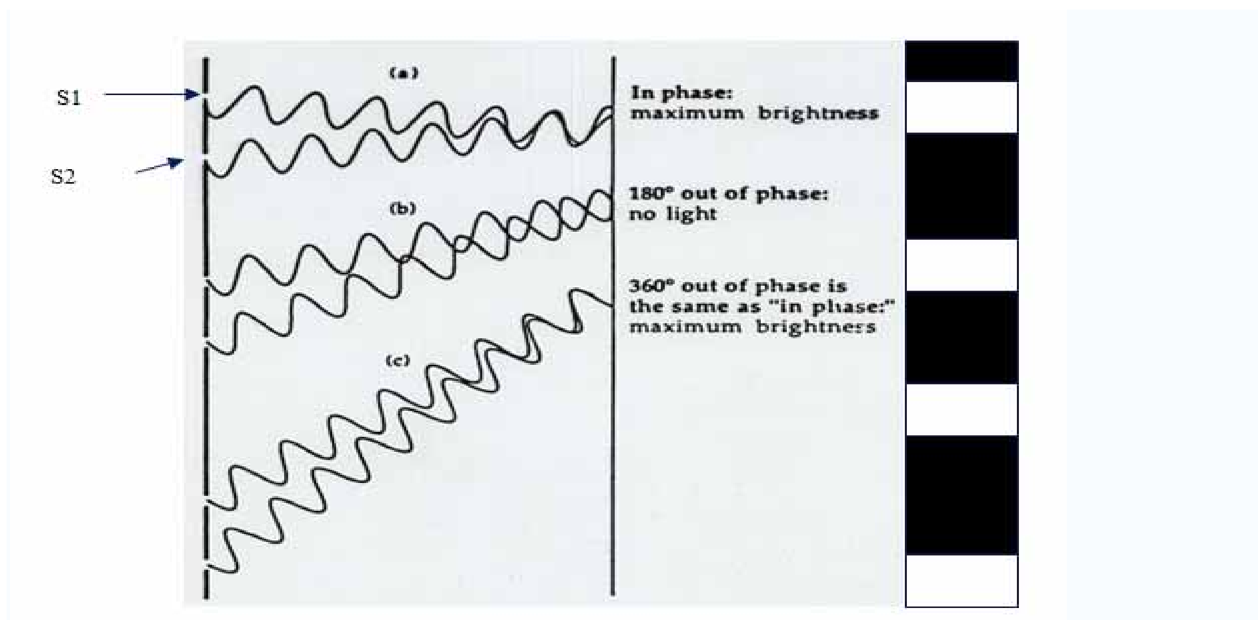

Figure 6. Formation of bright and dark streaks of light due to constructive and destructive interference of light waves. Adapted from [16].

Electron Diffraction

An ideal semiconductor crystal is composed of atoms arranged on a lattice defined by three fundamental translational vectors *a,b,c* such that the atomic arrangement looks the same in every respect when viewed from any point r as when viewed from the point *r'* [17] shown in Figure 7 and Figure 8,

$$\vec{r}' = \vec{r} + u\vec{a} + v\vec{b} + w\vec{c} \qquad (1)$$

where, u, v, w are arbitrary integers.

The set of points $\vec{r}'$ specified by (1) for all values of integers u, v, w define a lattice. A lattice is a regular periodic arrangement of points in space. The crystal structure is formed only when a basis of atoms is attached identically to each lattice point. The logical relation is,

lattice + basis = crystal structure (2)

The lattice and the translation vectors *a,b,c* are said to be primitive if any two points, *r, r'* from which the atomic arrangement looks the same, always satisfy (1) with a suitable choice of integers u, v, w. This definition of the primitive translation vectors guarantees that there is no cell of smaller volume that could serve as a building block for the structure. The crystal axes *a,b,c* form three adjacent edges of a parallelpiped. If there are lattice points only at the corners of the parallelpiped, then it is defined as a primitive parallelpiped. A lattice translation operation is defined as the displacement of a crystal parallel to itself by a crystal translation vector,

$$\vec{T} = u\vec{a} + v\vec{b} + w\vec{c} \qquad (3)$$

Any two lattice points are connected by a vector of this form and are shown in Fig 4.

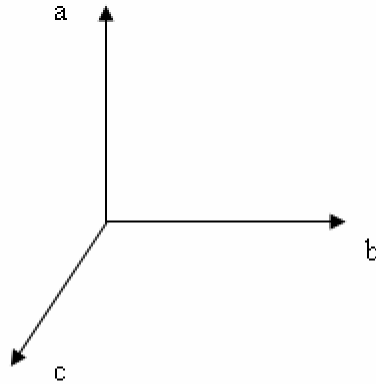

Figure 7. Crystal translational vectors a,b,c depicting the crystal axis in x,y,z directions. Adapted from [17].

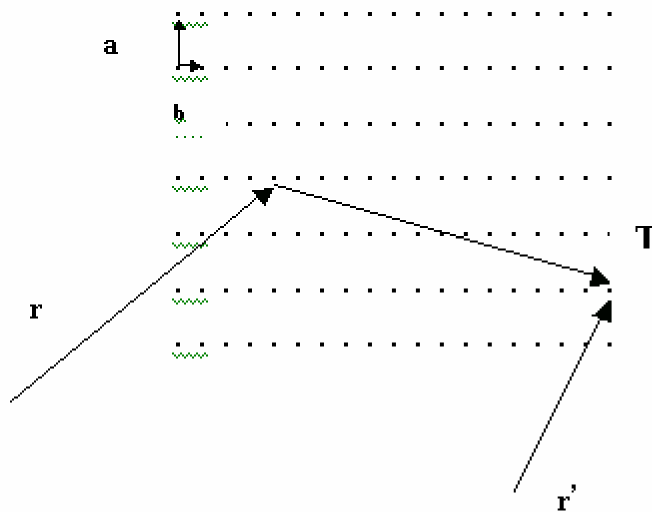

Figure 8. The above figure shows crystal lattice in a 2-dimensional space. The atomic arrangement in the crystal looks exactly the same to an observer at r' and r, provided that the vector T which connects r' and r may be expressed as an integral multiple of vectors a and b. Adapted from [17].

Attached to every lattice point there is a basis of atoms, with every basis identical in composition, arrangement and orientation. A crystal structure is formed by the addition of a basis to every lattice point. The lattice points are shown in Figure 9. The basis is indicated by dots in Figure 10. In Figure 11 the dots are omitted and each lattice point is replaced by the crystal basis.

The number of atoms in the basis may be as low as one, as for many metals and inert gases, but there are some structures for which the basis exceeds 1000 atoms. The position of the center of the atom j of the basis is given by,

$$\vec{r}_j = x_j\vec{a} + y_j\vec{b} + z_j\vec{c} \tag{4}$$

relative to the lattice point.

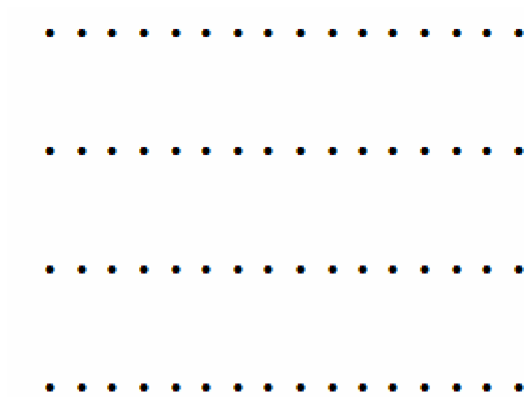

Figure 9. Space lattice. Adapted from [17].

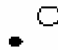

Figure 10. Basis, containing two different ions. Adapted from [17].

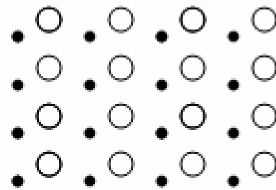

Figure 11. Crystal structure. Adapted from [17].

Equation (3) shows that a crystal is invariant under any translation of the form $\vec{T} = u\vec{a} + v\vec{b} + w\vec{c}$, where u, b, w integers and a, b and c are the crystal axes [17]. Any physical property of a crystal is invariant under T. The charge concentration, the electron number density, the mass density and the magnetic moment density are invariant under all translations T. Thus the electron number density $n(\vec{r})$ is a periodic function of $\vec{r}$ with a period *a,b,c* in the directions of the three crystals axes, whence $n(\vec{r} + \vec{T}) = n(\vec{r})$.

Most properties of a crystal can be related to the Fourier components of the electron density [17]. Consider a function $n(x)$ with a period '*a'* in one dimension. Expanding $n(x)$ in a Fourier series of cosines and sines:

$$n(x) = n_0 + \sum_{p>0} \left[C_p \cos\left(2\pi px/a \right) + S_p \sin\left(2\pi px/a \right) \right] \tag{6}$$

Where, the *p*'s are positive integers and C_p and S_p are real constants, called the Fourier coefficients of the expansion. The factor $2\pi / a$ in the arguments ensures that $n(x)$ has a period *a*:

$$\begin{aligned} n(x+a) &= n_0 + \sum_{p>0} \left[C_p \cos\left(2\pi px/a + 2\pi p \right) + S_p \sin\left(2\pi px/a + 2\pi p \right) \right] \\ &= n_0 + \sum_{p>0} \left[C_p \cos\left(2\pi px/a \right) + S_p \sin\left(2\pi px/a \right) \right] \\ &= n(x) \end{aligned} \tag{7}$$

Here, $2\pi / a$ is a point in Fourier space or in other words a point in the reciprocal lattice of the crystal. In one dimension these points lie on a line. The reciprocal lattice points tell us the

allowed terms in the Fourier series (6). A term is allowed if it is consistent with the periodicity of the crystal, as in Figure 9, other points in the reciprocal space are not allowed in the Fourier expansion of a periodic function.

Equation (6) can be rewritten as [17],

$$n(x) = \sum_{p} n_p e^{i2\pi p/a} \tag{8}$$

where the sum is over all integers p:positive, negative and zero. Extending the analysis to three dimensional lattice structures, equation (8) can be written as,

$$n(x) = \sum_{p} n_{\vec{G}} e^{i\vec{G}\cdot\vec{r}} \tag{9}$$

where $\vec{G}$ is called the reciprocal lattice vector and is given by,

$$\vec{G} = h\vec{A} + k\vec{B} + l\vec{C} \tag{10}$$

$$\vec{A} = 2\pi \, \vec{b}\times\vec{c} \big/ \vec{a}\cdot\vec{b}\times\vec{c}\,; \quad \vec{B} = 2\pi \, \vec{c}\times\vec{a} \big/ \vec{a}\cdot\vec{b}\times\vec{c}\,; \quad \vec{C} = 2\pi \, \vec{a}\times\vec{b} \big/ \vec{a}\cdot\vec{b}\times\vec{c} \tag{11}$$

Where, *h, k, l* are integers. Any arbitrary set of primitive vectors a, b, c of a given crystal lattice leads to the same set of reciprocal lattice points given by equation (10). Any vector $\vec{G}$ of this form is called a reciprocal lattice vector.

Every crystal structure has two lattices associated with it, the crystal lattice and the reciprocal lattice. A diffraction pattern of a crystal is a map of the reciprocal lattice, of the crystal, in contrast to a microscope image, which is a map of the real crystal structure. The two

lattices are related by the definitions (11). When the crystal is rotated, both the direct lattice and the reciprocal lattice are rotated. Vectors in the lattice have dimensions of [length]; vectors in the reciprocal lattice have the dimensions of $[\text{length}]^{-1}$. The crystal lattice is a lattice in real or ordinary space; the reciprocal lattice is a lattice in the associated Fourier space. A helpful tool for drawing the diffracted pattern is the Ewald's construction shown in Figure 12.

The spots on the right hand side and the reciprocal lattice rods represent the diffraction pattern in the reciprocal lattice space. The vector K is drawn in the direction of the incident electron beam and it terminates at any reciprocal point. A sphere is drawn with a radius equal to $k=2\pi/\lambda$ about the origin of K. The diffracted beam will be formed if this sphere intersects any other point in the reciprocal lattice. The sphere as drawn intercepts a point connected with the end of K by a reciprocal lattice vector G. The diffracted beam is in the direction $K_i=K+\Delta k$ where $\Delta k= G$. The construction was demonstrated by P.P.Ewald [17]. This is because after the completion of the growth the sample is smooth and uniform causing 2-dimensional diffraction to occur. The diffraction spots in the reciprocal lattice space are therefore close to each other and appear in the form of rods or streaks on the screen.

The RHEED patterns are therefore a symbolic representation of the surface morphology of a crystal. These patterns need to be recorded to observe and record the crystal growth pattern. These pictures can then be used for future studies to grow required semiconductor materials. First a single sample can be grown and the RHEED images can be recorded. When it is required to start mass production of the same semiconductor material these RHEED images can be used to compare and predict the growth of the crystals being grown. If the samples under mass production have RHEED images different from the earlier recorded ones, these can be discarded

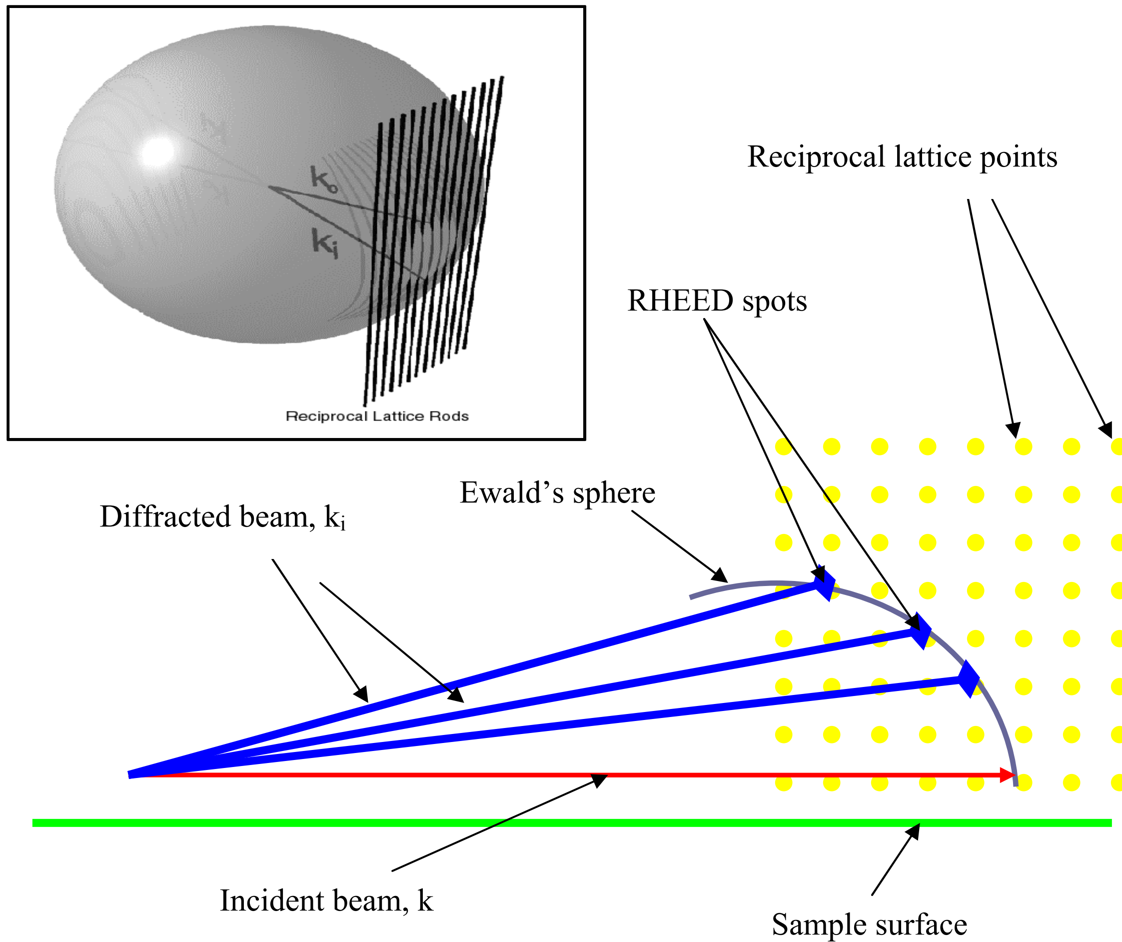

Figure 12. Ewald's sphere for the construction of diffraction pattern in reciprocal lattice space. Adapted from [17].

or the growth conditions be altered to achieve the required growth. By discarding the bad materials the cost and time involving in mass production of semiconductor materials is reduced significantly. New semiconductor materials can be grown in the place of defective samples thereby increasing the final quality and throughput of the mass produced semiconductor devices resulting in increased revenues and consumer satisfaction.

Reflection High Energy Electron Diffraction

The intensity of the RHEED oscillations also varies during the growth. When a layer

starts it has a smooth surface and the incident electrons undergo minimum diffraction when they are incident on the surface of a sample. Consequently the RHEED pattern is bright and has maximum intensity. As the layer nucleates, islands form on the surface, and the electrons undergo maximum diffraction leading to decrease in the RHEED pattern intensity. As the layer finishes, the islands coalesce into a flat layer, and the intensity of the RHEED pattern increases. Therefore, the period of one oscillation corresponds exactly to the growth of one monolayer of the semiconductor material during the growth [12]. RHEED is therefore used to calibrate growth rates, observe removal of oxides from the surface, calibrate the substrate temperature and monitor the arrangement of the surface atoms and to give a feedback on surface morphology during growth.

CHAPTER III

METHODOLOGY/ACQUISITION OF DATA

This chapter consists of two main sections: (a) Preparing the III/V chamber for growth and (b) Experimental setup for image capture and analysis.

The first section discusses in detail as to how the III/V molecular beam epitaxy (MBE) system is setup for growing wafers and the second section describes how the PCI-1409 frame grabber card is interfaced to the computer using the LabVIEW® software[*] to capture the reflection high-energy electron diffraction (RHEED) images of the sample being grown.

Preparing the III/V Chamber for Growth

The III/V and group IV MBE chambers present in the physics lab at UNT are shown in Figure 13 and Figure 14, respectively. Before the beginning of this thesis, the III/V chamber [18] had not been used for any type of growth for the past 5 years. This had led to the accumulation of residues such as carbon, arsenic, oxygen, nitrogen, gallium and water from the previous growths. The sample holders had also been left in the chamber for a long time, resulting in the deposition of unwanted residues on the surface of the sample holders. The view ports of the III/V chamber are also unclear, blocking the view of the load-lock, preparation and growth chambers for observation during the growth. The view ports, sample holders have to be cleaned using proper procedures before starting the growth. Secondly the crucibles which hold the individual materials such as Ga, As, P etc., that are used for depositing have also to be checked for residue material and it is to be determined if empty crucibles have to be filled with required materials. A step-by-step representation of the experimental procedure to set-up the III/V MBE system for

[*] National Instruments Corporation, http://www.ni.com/legal/termsofuse/unitedstates/us/

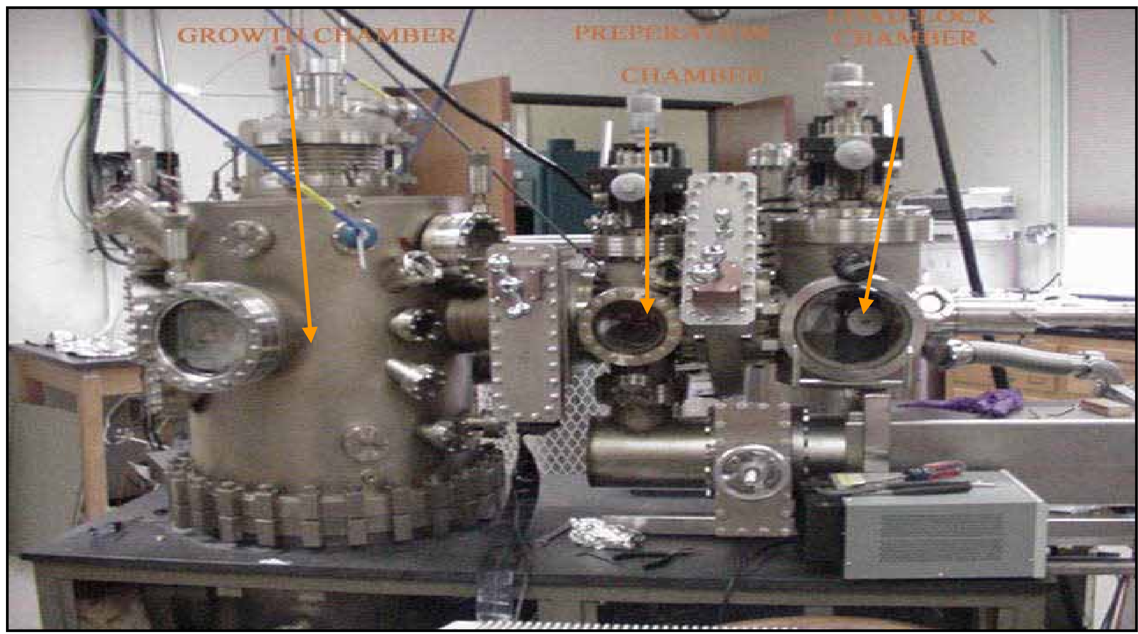

Figure 13. Varian 360, III/V MBE growth chamber at UNT.

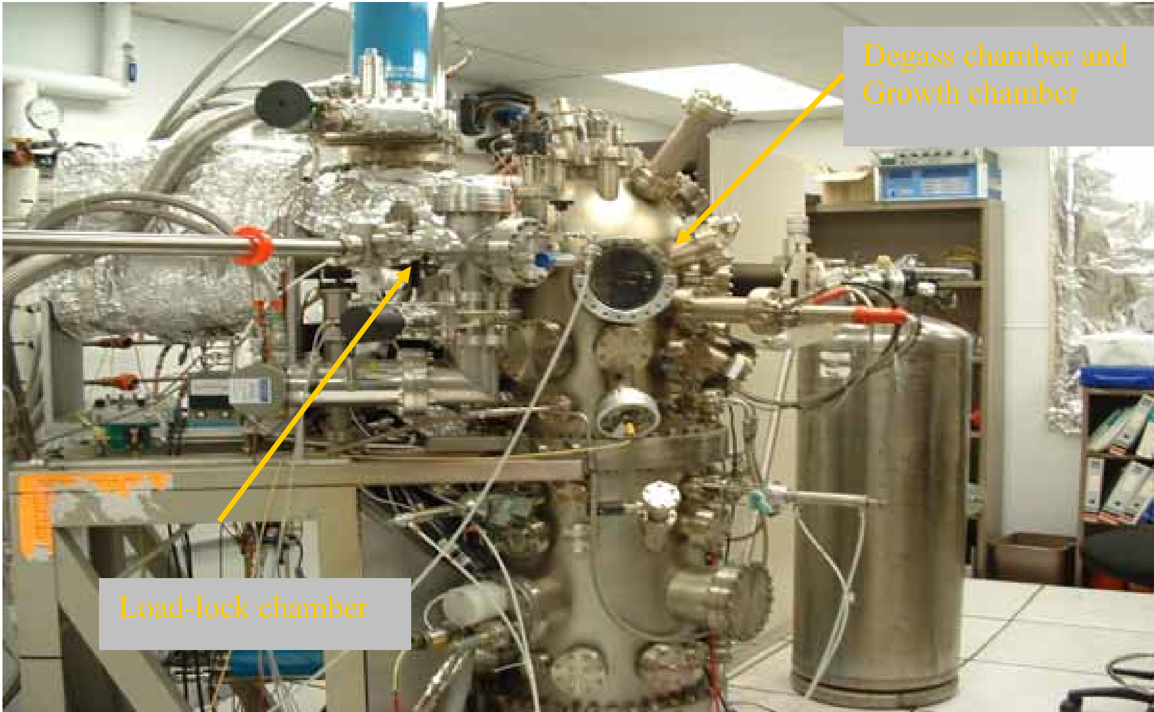

Figure 14. Group IV MBE system at UNT.

growth is shown in Figure 15. The MBE chamber is usually under very low pressures of the range of 10^{-8} to 10^{-10} Torr. The chamber should be bought to atmospheric pressure before performing any maintenance procedures. The different vacuum pumps operating on the system, shown in Figure 16 and Figure 17 are: mechanical pump (2); turbo pump (1); ion pump (3); and cryo-pump (1).

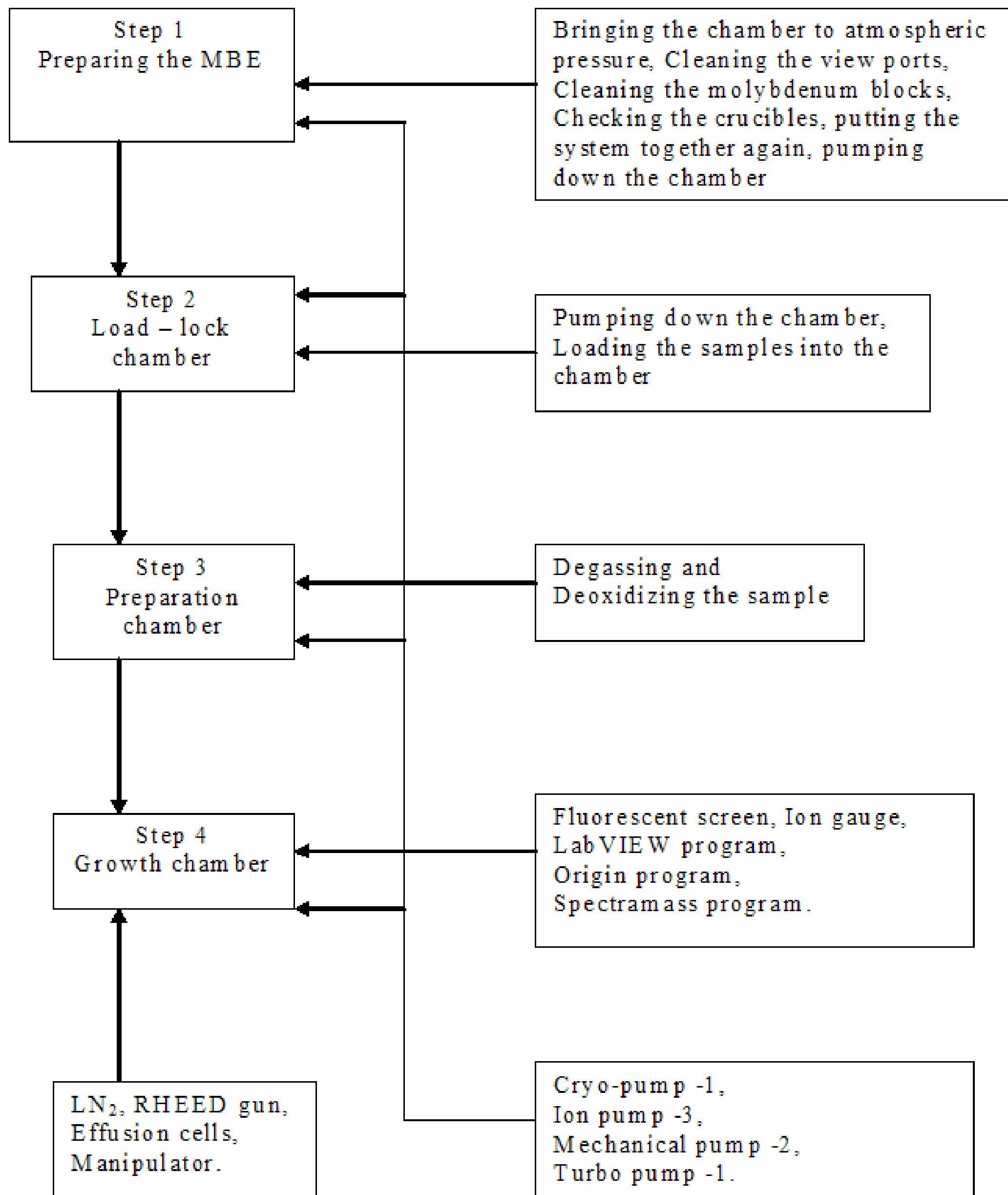

Figure 15. Flow diagram to represent the experimental procedure of the III/V MBE.

Figure 16. Vacuum pumps on the III/V MBE system.

The vacuum pumps are shut down one after another. Materials such as arsenic are poisonous, hence lab coats, face masks, head masks, hand gloves, protective eye glasses have to be worn before opening the system to avoid contact with any hazardous materials. The view-ports are cleaned first. A solution of H_2SO_4: H_2O_2: De-ionized water in the ratio of 1:2:10 is prepared before hand to clean the view ports as soon as they are removed from the MBE system. The view-ports are removed from the system from the MBE system so that the other side of the view-port can also be cleaned and the opening created on the MBE system because of this is covered with aluminum foil to prevent any dust particles or impurities entering the system. After detaching from the main system the view ports and cleaned repeatedly using the above prepared solution. It is not advisable to immerse the view ports in this solution because usage of this

solution in large amounts will etch away the glass on the view ports. Finally the view ports are rinsed with de-ionized water.

Figure 17. Ion pump and cryo-pump on the III/V MBE system.

After opening the view ports the substrate holders are removed from the system. The substrate holders used in this system are made of molybdenum. A solution of HCl:H_2NO_3:De-ionized water in the ratio of 1:2:1 is prepared and the molybdenum blocks are cleaned repeatedly using a wipe cloth. Finally the molybdenum blocks are rinsed in de-ionized water.

The screws of the crucible holders are undone and the crucibles are removed from their holders. The crucibles are made of high purity pyrolytic boron nitrate, extreme fine handling is required while undoing the screws and removing the crucibles from their holders. The crucibles are checked for any damage. If they are cracked or completed destroyed they are replaced by new ones. Good crucibles are checked if sufficient amount of semiconductor material is present in the crucibles, if not new material is ordered.

The linear transfer rod on the system is used to transfer the substrates from the loading chamber to the growth chamber. This rod has to be aligned in a straight line so that the substrates don't hit against the system walls during the transfer. There are four screws on the transfer rod for this purpose. The two screws on the top and bottom on the rod are used for vertical alignment. Two more screws on the right and left sides of the transfer rod are used for horizontal alignment. These screws are adjusted accordingly to correct any misalignment.

The samples used during the growth come in epi-ready form. The GaAs wafers were received in an epiready state, i.e., the surface was smooth enough to warrant an epitaxial growth, however, to ensure the optimal surface conditions the wafers are first cleaned in trichloroethylene, rinsed in methanol, and etched in 5:1:1 mix of $H_2O:H_2O_2:H_2SO_4$ for 3 minutes, then rinsed in running deionized (DI) water for 2 minutes and then blow dried with nitrogen. Cleaning of the sample results in the formation of a protective oxide layer on the sample. The samples are then mounted on the molybdenum block (or in short, moly-block) using indium. The loading chamber has a capability of holding 8 substrates at a time so, 8 moly-blocks are mounted with samples at a time and are kept ready for growth.

Preparing Samples for Growth

The cleaned view ports and any new components ordered for the system are put back on the system at this time. The isolation valves between the load-lock and preparation chamber, preparation and growth chambers are closed. The turbo pump and mechanical pumps are connected to the load-lock chamber. The turbo pump is used to pump down the load-lock chamber. When the pressure reaches approximately 10^{-1} Torr the turbo pump is shut down and the mechanical pumps are started at the same instant. When the pressure reaches approximately

10^{-4} Torr the isolation valves are opened and the entire system is allowed to pump down using the mechanical pumps for approximately 12 hours. Then the ion pumps and the cryo-pumps are turned on and the mechanical pumps are shut down. The system is pumped down using the ion pumps to the least achievable atmospheric pressure usually 10^{-10} to 10^{-12} Torr. The system is left to pump down for about 48 hours to create the UHV conditions.

After the required pressure is achieved, the load-lock chamber is isolated from the rest of the chamber and using the isolation valve present between the load-lock chamber and the preparation chamber, shown in Figure 18. It is then bought to atmospheric pressure. The moly-blocks are then mounted manually on the carousel holder, shown in Figure 19.

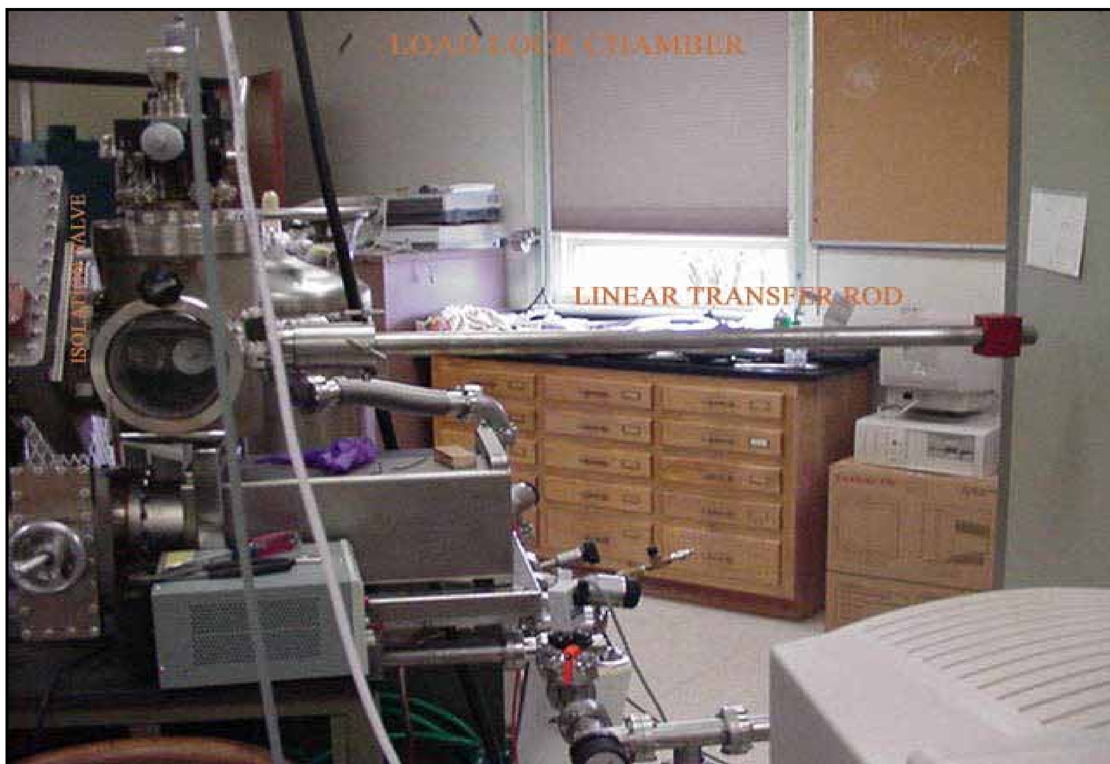

Figure 18. Load-lock chamber of the III/V MBE system.

Figure 19. View port of the load-lock chamber showing the molybdenum blocks and samples.

The view-port is closed again tightly and is pumped down using the mechanical and turbo pumps. This is done overnight. After this, the isolation valve between the load-lock and preparation chamber is opened and the system is again allowed to pump down to remove any pressure difference between the load-lock chamber and the main chamber. After this, the moly-blocks are transferred from the load-lock to the preparation chamber using the linear-transfer rod, one at a time. Now, the isolation valves between load-lock and preparation chamber, preparation and growth chambers are closed.

The sample is then heated in the preparation chamber. This heating process removes the protective oxide layer that was formed on the sample after the cleaning process. This process is also known as de-oxidation and is done by heating the sample to a previously calibrated temperature (e.g. ~600°C for GaAs) for a few minutes. In addition to these the samples may also contain carbon and hydrogen atoms as impurities. These can be removed by heating the sample to a previously calibrated temperature (e.g. 200°C for GaAs) in the preparation chamber and the process is known as degassing. Performing the degassing and deoxidation functions in the

preparation chamber prior to the sample growth in the growth chamber, primarily reduces the presence of impurities in the growth chamber. The preparation chamber is isolated from the growth chamber through another isolation valve as shown in Figure 20.

Figure 20. Preparation chamber of the III/V MBE system.

The growth chamber is where the final growth of the sample takes place. The schematic diagram of the growth chamber is as shown in Figure 21 [15]. This chamber houses the RHEED electron gun, fluorescent screen to observe the RHEED images, liquid nitrogen (LN_2) cryo-panels to circulate liquid nitrogen during growth, effusion cells with shutters, furnaces to heat the effusion cells, ion gauges to measure the chamber pressure, isolation valve between the growth chamber and preparation chamber, a manipulator, view port to observed the sample during growth. The thermal stability of the effusion cells is ensured by isolating them through LN_2

cooling. For this purpose the chamber has two built in cryoshrouds, one in the flange containing the cells and the other in the growth chamber. The cooling also served the purpose of reducing the pressure in the chamber, and thus, the amount of contaminants during the growth. The furnaces and the thermocouples, attached to the back of the crucibles are in closed loop configuration with temperature controllers, which kept the temperature. Separate controls exist for the RHEED gun and the manipulator outside the chamber. The samples are placed and withdrawn from the chamber using the linear transfer rod. The manipulator was mounted along a horizontal axis and it provided facility to automatically continuously rotate and heat the substrate. The substrate can be positioned, with respect to the beam sources, at any angle between horizontal and vertical. It also includes, X, Y, Z motions, thus allowing the RHEED beam incidence angle to be varied. The manipulator has a non-inductively wound high efficiency Tantalum(Ta) radiation foil, which allows substrate heating to temperatures up to 800°C.

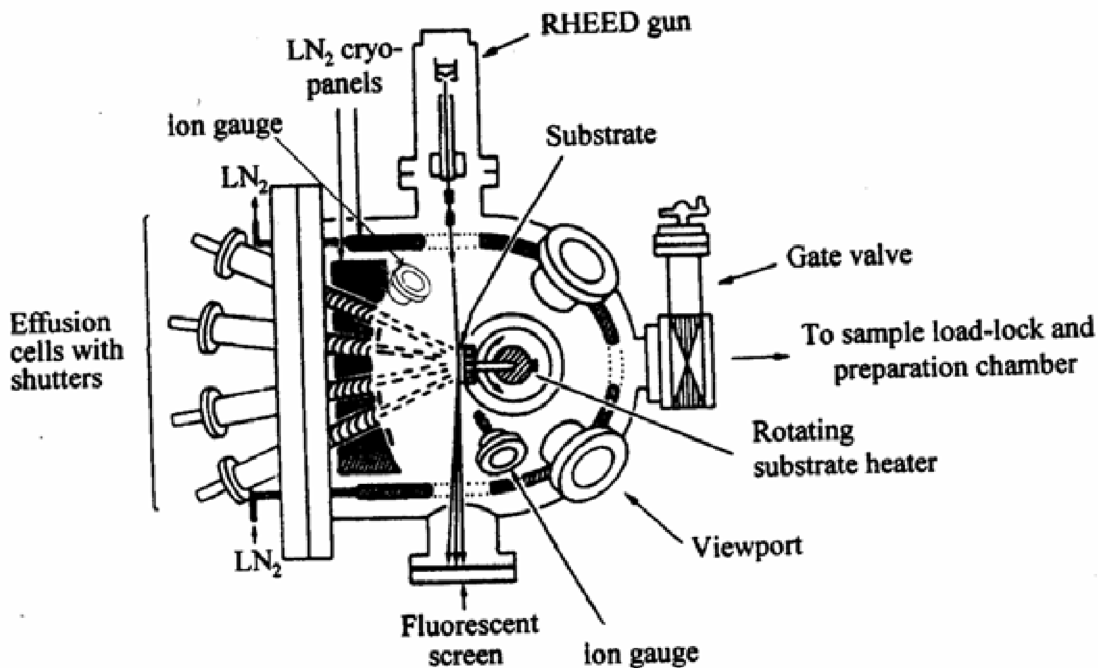

Figure 21. Top view of a typical standard MBE system growth chamber [15]. Reproduced with permission from Springer Science and Business Media.

The Varian MBE 360 growth chamber is as shown in Figure 22. There are 7 effusion cells in this chamber, one each for Bi, Al, As, In, P, Sb and Ga. The RHEED gun is operated typically at 9.5KeV. After the sample is deoxidized and degassed in the preparation chamber, the isolation valves are opened and the sample is transferred to the growth chamber using the linear transfer rod. The growth chamber has a manipulator, which has an arrangement to hold the moly-block. After the transfer is complete the linear transfer rod is removed from the growth and preparation chambers and is pulled out all the way back to the load-lock chamber. The isolation valve between the growth chamber and the preparation chamber is then closed. The individual effusion cells are heated using furnaces for depositing the materials on the sample. For practical growth, the recommended substrate temperature for MBE for GaAs ranges from 500 to 630°C [20]. The shutters can be opened and closed manually by using the Shutter Control switches shown in Figure 22. Liquid nitrogen is circulated around the growth chamber during the growth, to isolate the temperatures of the individual effusion cells from each other and to maintain appropriate growth temperature in the chamber. During deposition the diffracted electrons from the surface of the sample can be observed on the phosphor screen, shown in Figure 22.

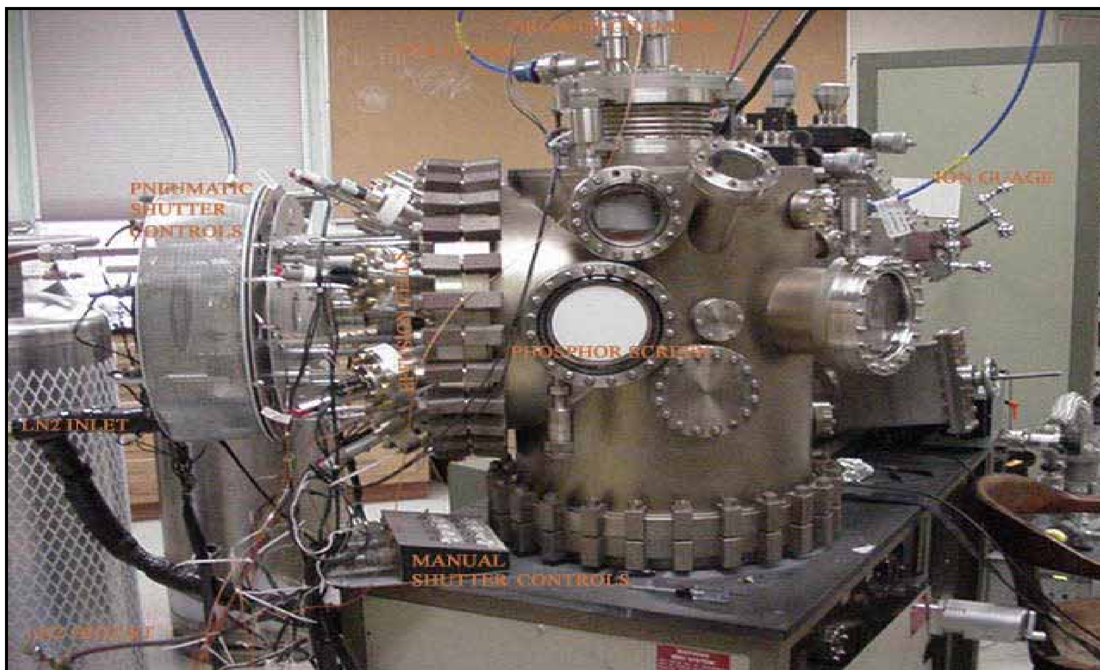

Figure 22. Growth chamber of III/V MBE system.

Figure 23. Screen shot of the SpecView program.

The SpecView software that came with the MBE equipment, was already installed and working before getting started on the LabVIEW® program. Using this software, the current

temperature of the source cells and the substrate can be observed and changed. Figure 23 shows 8 rectangular blocks for each control. Each rectangular block shows two different values of temperatures. The top value is specified by the user i.e., the required temperature that is required and can be entered using the keyboard, the bottom value is the current temperature being read by the controller and changes continuously. When the user enters the required value, the SpecView Software sends signals to the PID (Proportional Integral Derivative) controllers [21], which apply current to the furnaces to control the furnace temperatures of the effusion cells and the substrate The temperature of the effusion cells can also be controlled manually, the control rack which houses the controls panels and equipment for this purpose is shown in Figure 24. Each control panel has individual push buttons to increase or decrease the temperature manually.

Figure 24. Furnace control unit housing rack.

RHEED control Equipment housing rack is housed in a separate rack as shown in Figure 25. The voltage and the current to the electron gun can be controlled using this control unit. This unit also consists of control units for ionization gauge and the manipulator control.

Figure 25. RHEED control Equipment housing rack.

Experimental Setup for LabVIEW®

Until now the process of setting up the MBE system to grow wafers has been discussed. Now, the experimental setup to capture the RHEED images shall be described.
This will include a description of the hardware used to capture the RHEED images and a description of the LabVIEW® program needed to interface the hardware to the computer to capture the RHEED images and the necessary data.

PCI-1409 Frame Grabber Card

The hardware device used for interfacing the video signals obtained from the RHEED camera source is the PCI-1409 frame grabber card shown in Figure 26 [22], designed by National Instruments. The PCI-1409 frame grabber is a high-accuracy, monochrome and Image Acquisition (IMAQ) board for PCI chassis that support RS-170, CCIR, NTSC and PAL video standards as well as some nonstandard cameras from any of four input sources. The board features a 10-bit analog-to-digital converter (ADC) that converts video signals (RHEED intensity values) to digital formats. The PCI-1409 acquires images in real time and can store these images in onboard memory or transfer these images directly to system memory. The 1409 device is simple to configure using the LabVIEW®, National Instruments-Image Acquisition (NI-IMAQ) software from National Instruments. The 1409 device supports four general purpose control lines that can be configured to generate precise timing signals for controlling camera acquisition. The device also supports four video sources and four external I/O lines that can be used as triggers or digital I/O lines. The device can acquire at a rate of 30frames/second with a RS-170/NTSC compatible camera, 25frames/second with a CCIR-60/PAL compatible camera and 60frames/second with a double-speed progressive scan camera.

Figure 26. PCI-1409 frame grabber card supplied by National Instruments [22].

The experimental setup for capturing the RHEED images is shown in Figure 27. The camera is placed in front of the phosphor screen of the III/V MBE system. The camera is connected to the PCI-1409 frame grabber card using a Bayonet Neill-Concelman (BNC) connector. The frame grabber is installed in a PCI slot of a computer that has the LabVIEW® code installed in it. During the growth process the camera is switched on and the LabVIEW® code are run simultaneously to record the RHEED images and intensities. A detailed description of the LabVIEW® code will be given next.

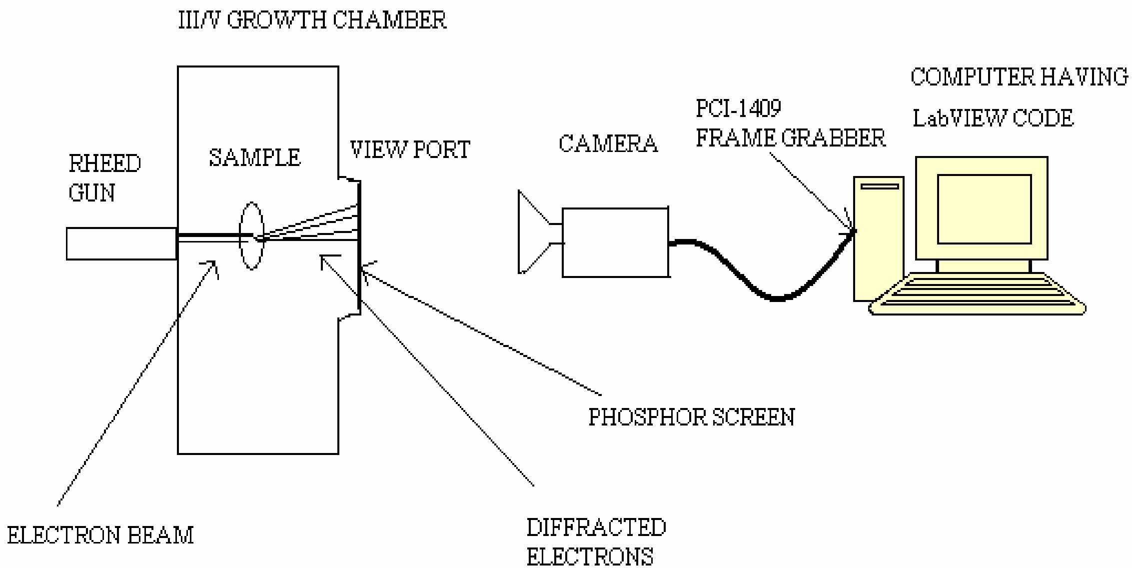

Figure 27. Experimental setup to capture RHEED images of the III/V MBE chamber using the LabVIEW® code.

Figure 28 shows step-by-step sequence in which LabVIEW® program is executed. The LabVIEW® code is written as a 6 step sequence, the program proceeds from one sequence to other automatically and in LabVIEW® the first sequence number start from 0.

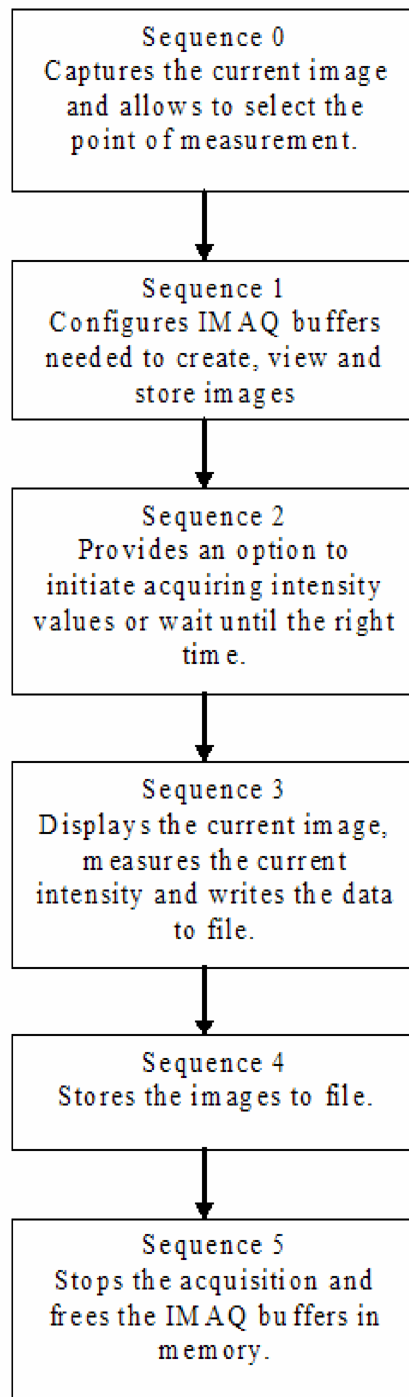

Figure 28. Flow diagram depicting the functioning of the LabVIEW® code.

LabVIEW® user interface screen for the model is shown in Figure 29. It consists of various numeric controls and indicators. It also has graphical interface to observe variations

graphically. The name of the image, chart can be chosen using the control inputs such as 'Image Name', 'Chart Data' [23]. These values are initialized before the acquisition starts. The data can be written to a new file or appended to a current file by selecting the 'Append to File' option. When this button is enabled the data that will be recorded next run will be written to a new file, if not it will be written to the file where the data was written in the last run. The data can be transposed before saving to the file switching the 'Don't Transpose' control to 'Transpose' option.

The PCI-1409 is interfaced to the program under the 'Interface Name' and 'Interface Name 1' at various stages of the program. Here, the interface name is 'img0'. The number of bytes used to encode the image is selected using the control 'Image Type'. In IMAQ, image buffers have to be created before an image is created. When the images are captured, they are stored in these buffers. When the buffer space becomes saturated the oldest image is discarded and the incoming image is stored. This procedure takes place as long as the image acquisition takes place. The number of image buffers needed is specified before the acquisition using the 'Number of buffers' control. The point at which the intensity measurements are made on the image is stored is indicated under the indicator 'POINT'. This point can be shifted during the acquisition process using the 'Coordinate System' control. In this control the 'Reference System' indicates the current X and Y co-ordinates on the chart where the measurement is being made. The 'Measurement System' values indicate the final co-ordinates where the point of measurement has to be shifted. When the Measurement System co-ordinates are entered, the measurement point automatically shifts by the difference between the Reference System and Measurement System. The 'Start' button starts the acquisition. The 'See Images button provides the option of viewing the images continuously as the acquisition takes place. The 'Stop' button

stops the acquisition. The 'Gray Level Intensity' indicator indicates the intensity at the point of measurement on the image.

The intensity values are plotted continuously during the acquisition on the 'Waveform Chart', shown in Figure 30. The intensity values are plotted on Y-axis and the time is plotted on X-axis. These values are also indicated using the arrays, 'Amplitude' and 'Chart-Time' respectively and are shown in Figure 31. The 'Error Out' indicators numbered from 1-7 displays an error message when an error occurs during the execution of the program.

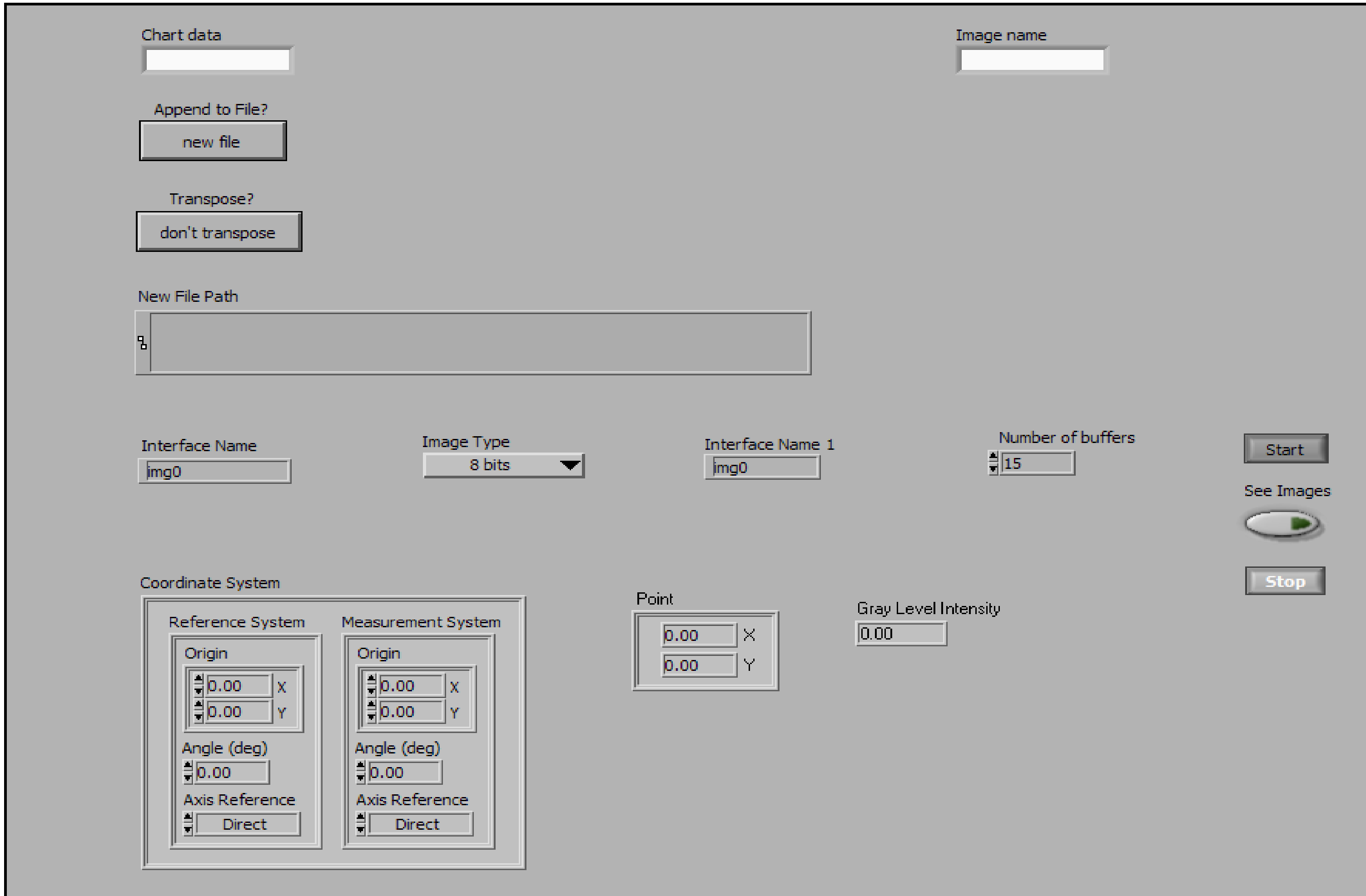

Figure 29. Front panel showing the various controls for the program.

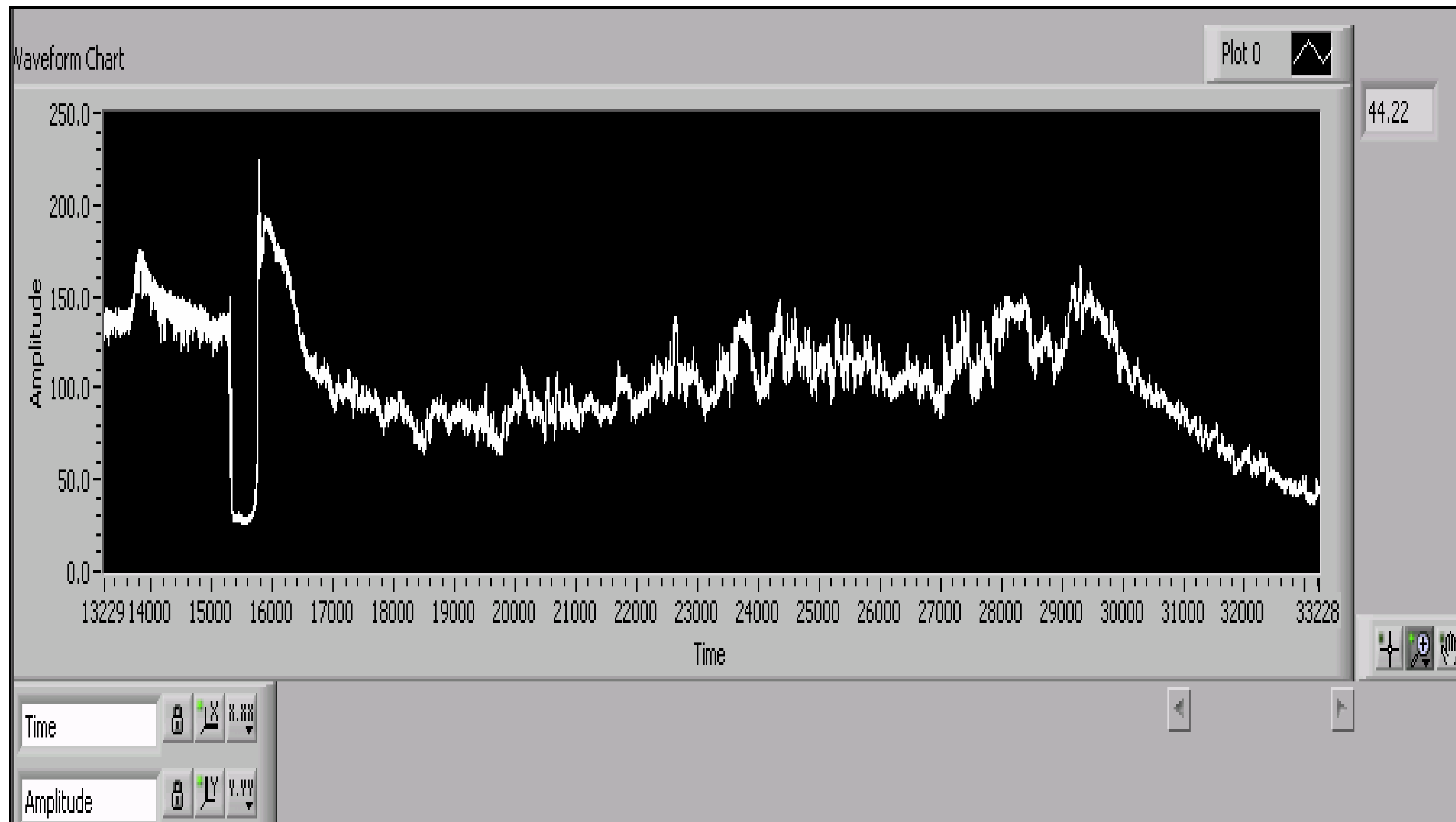

Figure 30. Front panel showing the Waveform Chart.

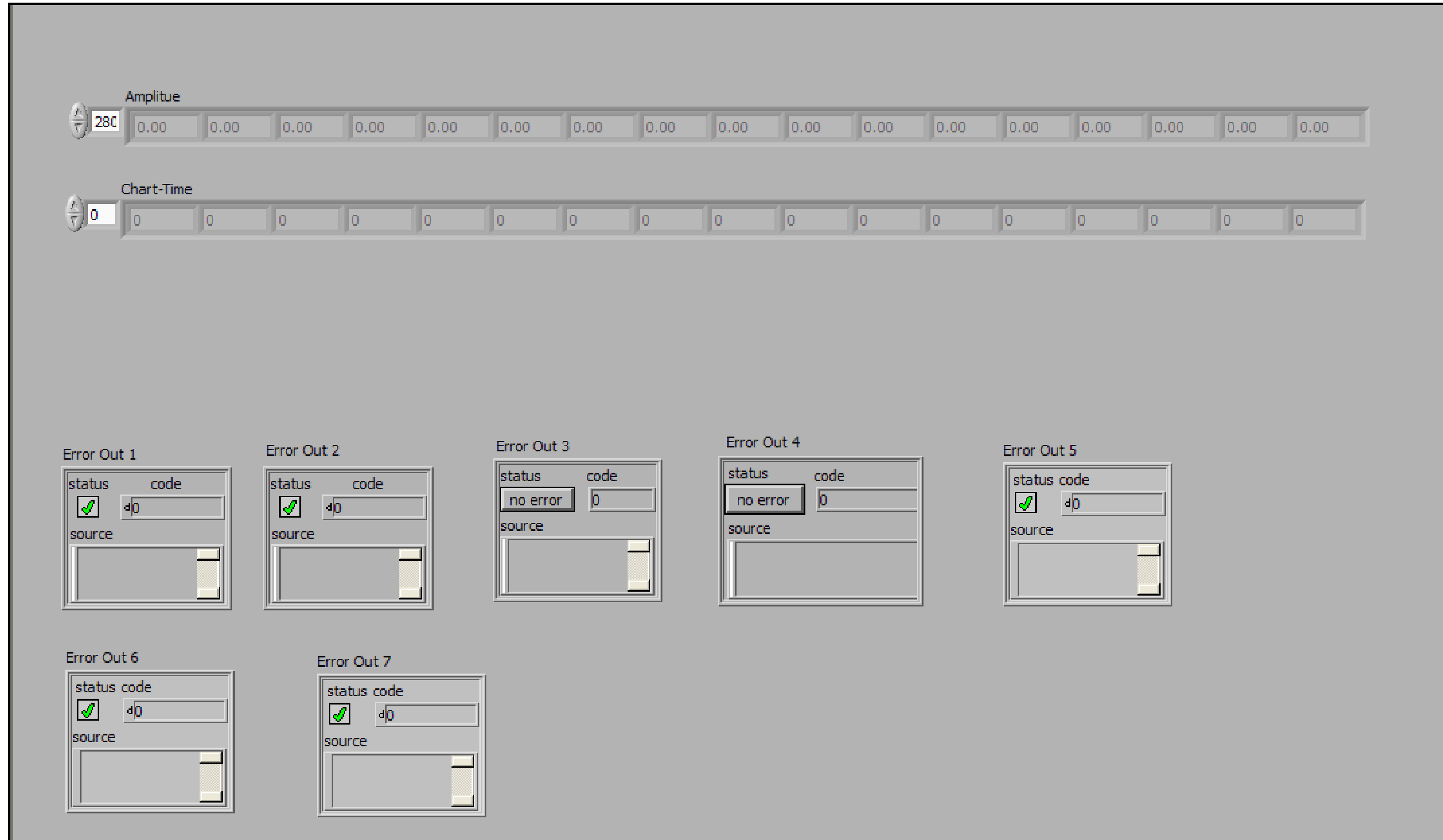

Figure 31. Front panel having the ERROR INDICATORS at various stages of the program.

The following description explains the backend LabVIEW® program. The first sequence (Sequence 0), is specifically aimed at deciding the point at which the measurement is made on the image. IMAQ INIT.VI initializes the image capture by connecting to the PCI-1409 board and IMAQ SNAP.VI snaps the current image and displays it on a separate window. This image is then opened using the IMAQ SELECT A POINT.VI which is used to select the required point on the image. The location of this point is stored as a numeric value labeled 'Point', shown in Figure 32. At the end of this sequence, the image is disposed using the IMAQ DISPOSE.VI, but the point at which the measurements are to be made is stored.

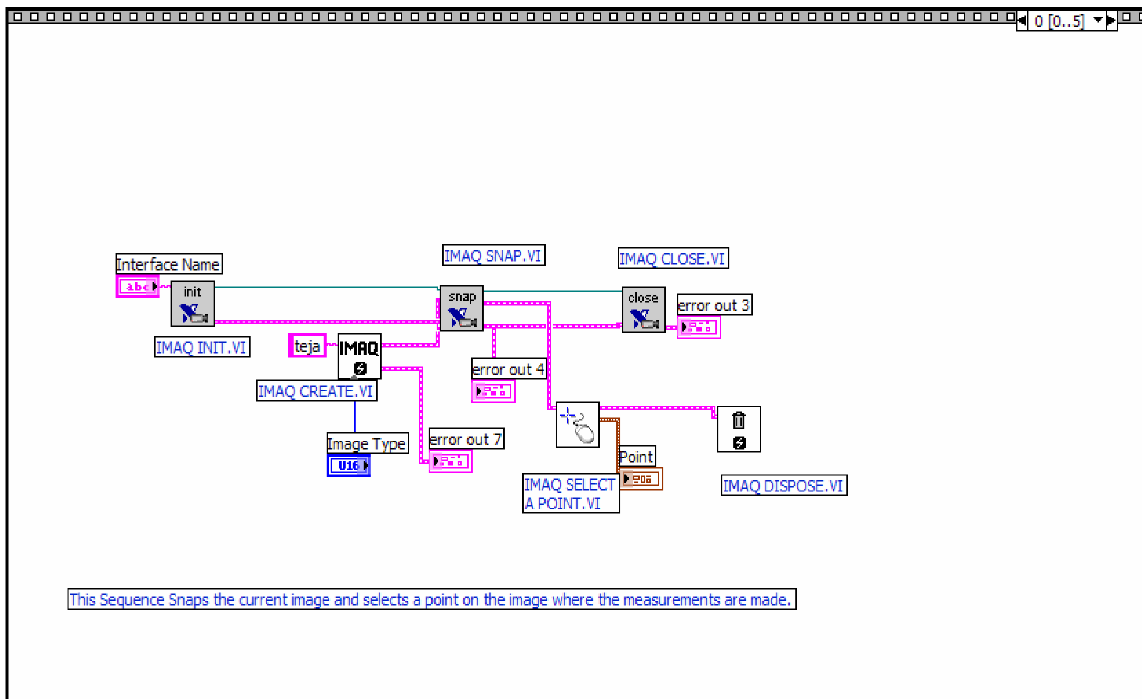

Figure 32. Sequence 0, used to select a point on the image at which the measurements will be taken.

The second sequence (Sequence 1), shown is Figure 33 configures the buffers required to create and view the images. The configuration is initialized using IMAQ INIT.VI [24]. The user can choose to do either a continuous acquisition or one shot acquisition using IMAQ

CONFIGURE LIST.VI. This VI also provides a choice for on-board memory storage or system memory storage. For this program continuous acquisition is chosen and the images are saved on the system because continuous capturing and storage of images is required for the experiment. The memory buffers are then allocated using IMAQ BUFFER LIST.VI.

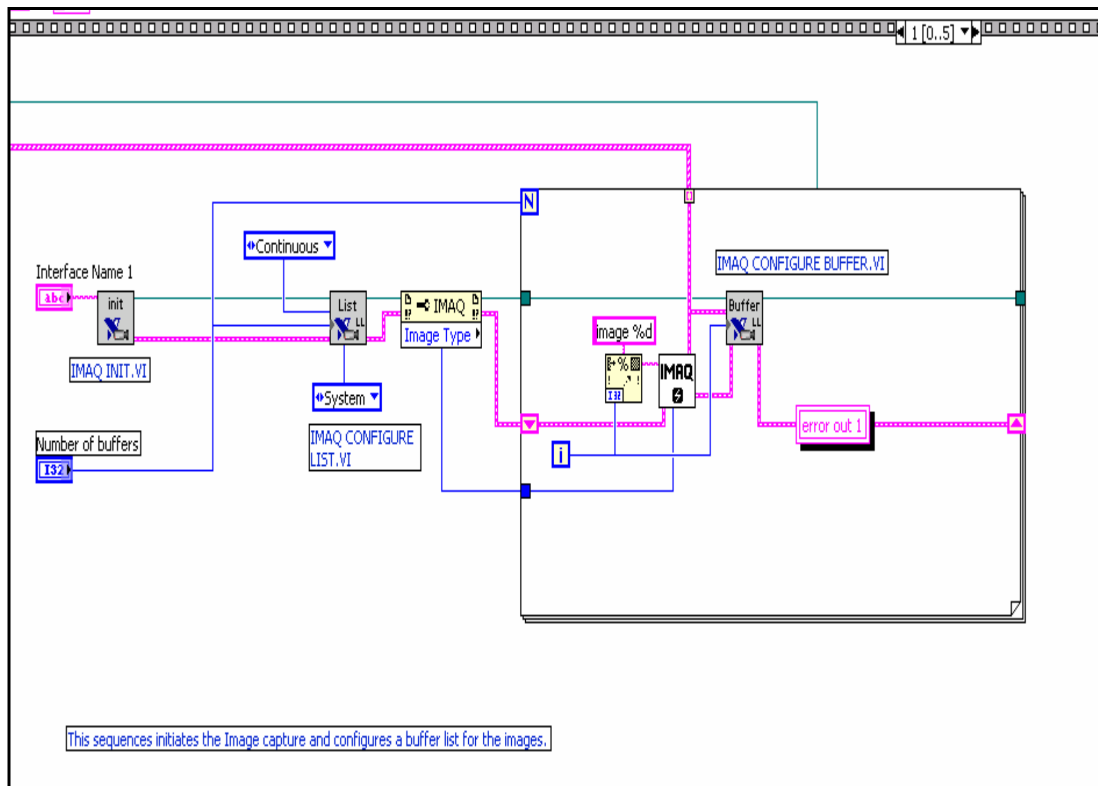

Figure 33. Sequence 1, configuring IMAQ buffers for acquisition.

In the third sequence (Sequence 2), shown in Figure 34, the program waits until the 'START' button is enabled to initiate the next sequence. This is the point at which after the image buffers have been configured and the program is initialized for RHEED image capture, the user has a choice to start the acquisition immediately or wait until a particular time during the growth. Once the 'START' button is enable the program proceeds to next sequence.

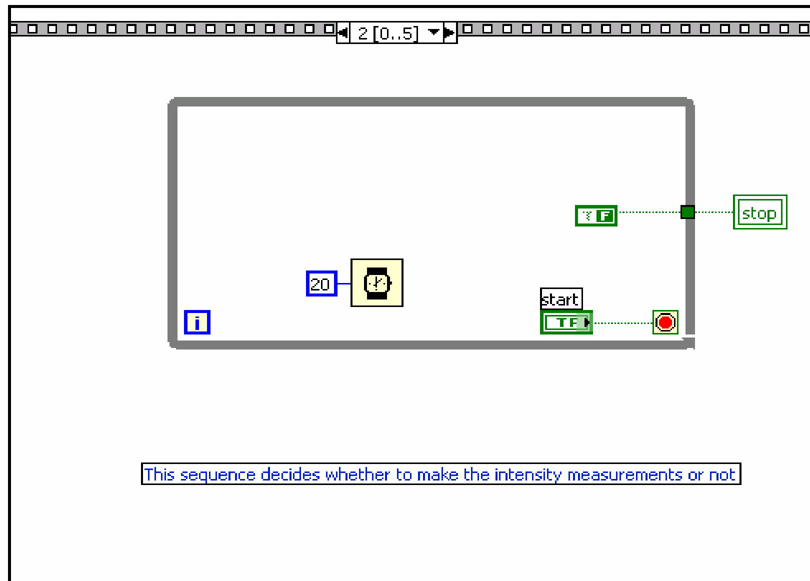

Figure 34. In Sequence 2, a decision is made whether to start the acquisition or to wait further.

The fourth sequence (Sequence 3), shown in Figure 35, performs the function of displaying an image using the IMAQ WINDRAW.VI, when the SEE IMAGES button is activated on the front panel. The image is displayed in a separate window using the IMAQ WINDRAW.VI continuously. The sequence also initiates a For-loop which makes use of the IMAQ LIGHT METER.VI to measure the intensity of the incoming images. The For-loop keeps on running until the 'STOP' button on the front panel is enabled. IMAQ LIGHT METER.VI makes use of the numeric value stored as 'Point' during sequence '0'to measure the intensity at a specified point. The values are also plotted on a chart continuously. A 'Wait Until next ms' Timer is assigned a constant of 50 so that a time difference of 50ms is maintained between each measurement.

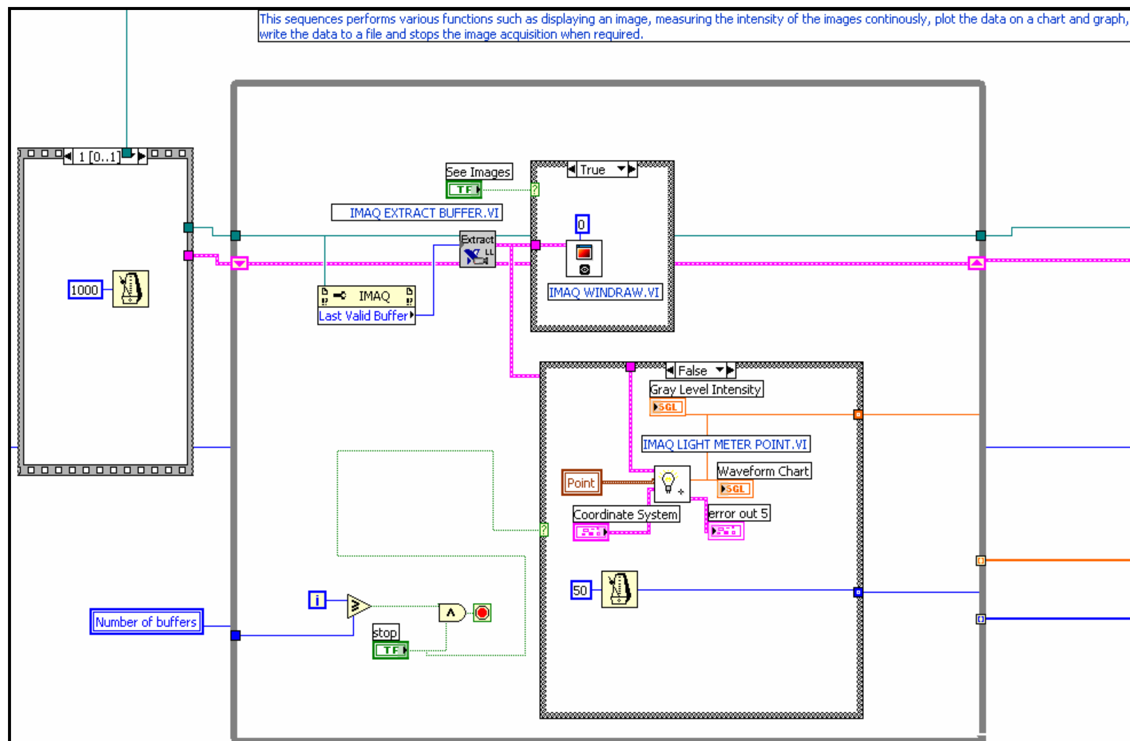

Figure 35. Sequence 3 displays an image and measures the intensity on the image.

The remaining part of Sequence 3, shown in Figure 36, saves the chart data to file. ‘WRITE TO SPREADSHEET FILE.VI’ opens a pop-up window giving the user an option to select the name of the file and the location at which the data is stored. The data is stored as an EXCEL file. Also, during every run sequence the data can be stored to a new file or appended to an existing file. This can be done by enabling the ‘Append to File’ button on the front panel. When the ‘STOP’ button on the front panel is activated the For-loop stops running and IMAQ STOP.VI stops the current acquisition on the IMAQ device. The program then proceeds to Sequence 4.

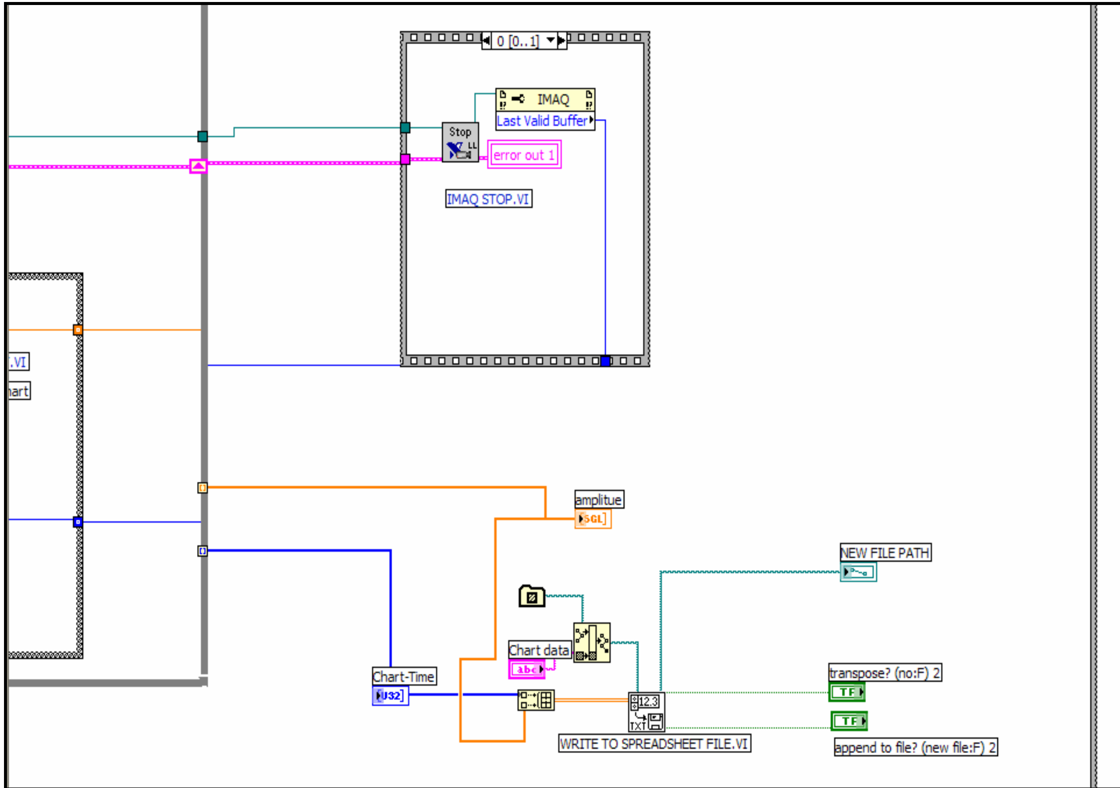

Figure 36. Sequence 3 also stops acquisition and writes the data to file.

In the fifth sequence (Sequence 4), shown in Figure 37, FILE DIALOG.VI then opens a pop-up window asking the user to select the directory where the images can be stored. The images are saved to file using the IMAQ WRITE FILE.VI and the acquisition is closed using IMAQ CLOSE.VI and system resources allocated during the acquisition are released.

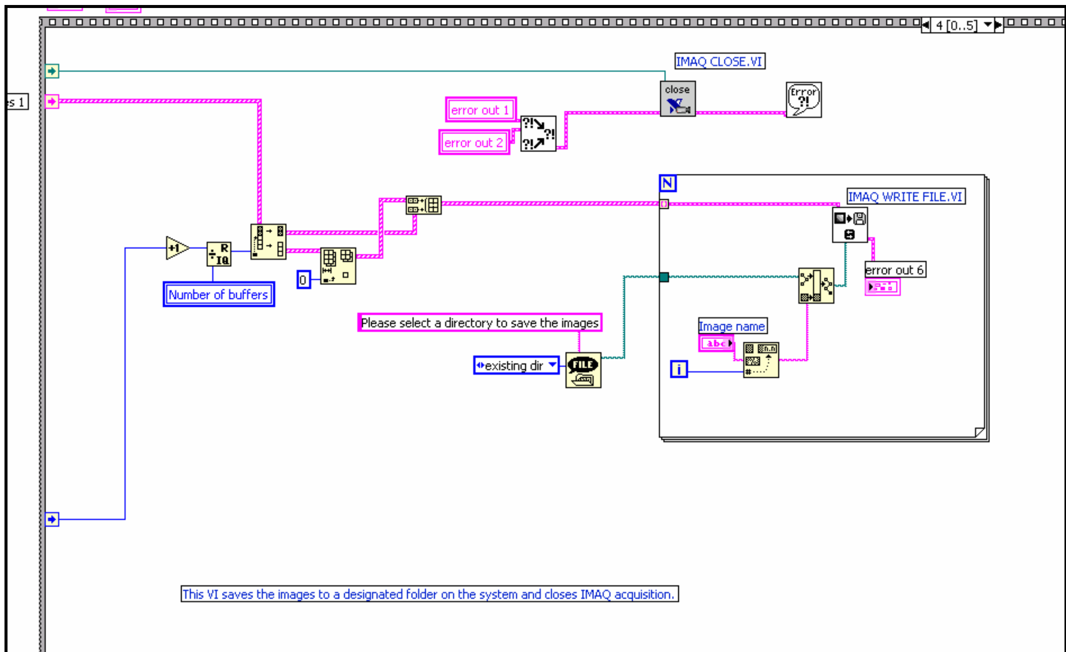

Figure 37. Sequence 4 writes images to file.

The sixth sequence (Sequence 5), shown in Figure 38, releases the buffers in the system memory using the IMAQ DISPOSE.VI to the end of the program.

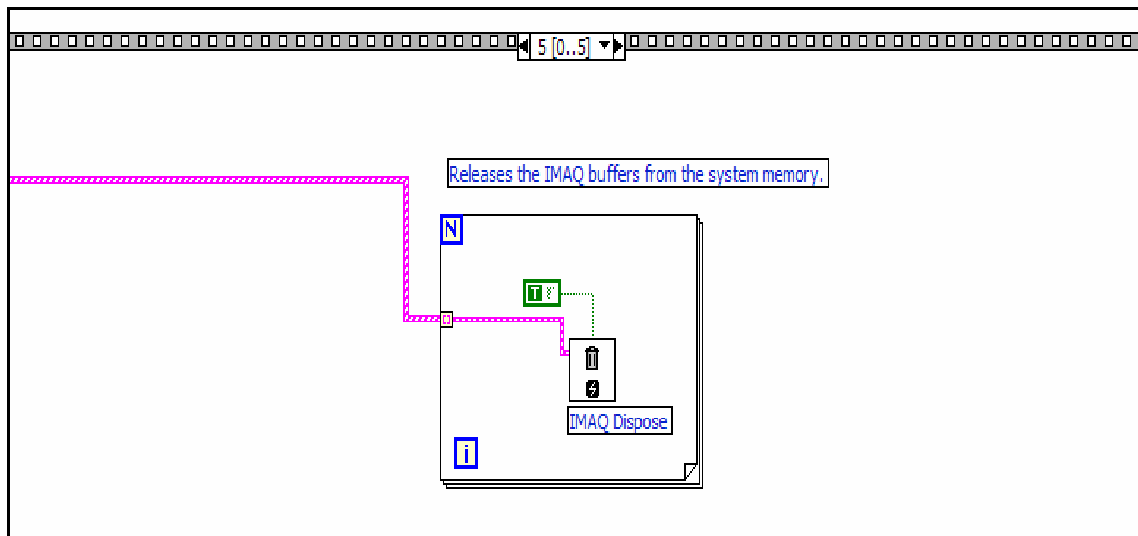

Figure 38. Sequence 5 closes the acquisition and releases IMAQ buffers in system memory.

CHAPTER IV

RESULTS AND DISCUSSION

This chapter focuses on the readings obtained and their analysis on the samples grown on the group IV molecular beam epitaxy (MBE) system. When the epiwafer is being grown, the readings are taken from two different software programs simultaneously. One, the LabVIEW® program[*] which is under test and the other is the Dr.Gossmann's program, which is currently deployed on the group IV system. These two readings will be compared later to verify the proper functioning of the LabVIEW® program under test.

For the first sample, a silicon (Si) wafer was chosen. A layer of Si was deposited on the wafer by heating the Si source cell to 500°C, for 30 min. Then a layer of Iron (Fe) was grown for approximately 5 min at 600°C and the readings were taken. . For simplicity the growth pattern for this recording is referred to as sample-1. The graph obtained using LabVIEW® is shown in Figure 39. After this the Fe is deposited at 650°C and the oscillations are recorded. These oscillations are appended to the same graph. Here the data is appended to the same graph to observe the difference in oscillations clearly. This sample is called sample-2. Figure **40** shows the reflection high-energy electron diffraction (RHEED) image for sample-1 before the deposition of Fe on a Si wafer. The resulting sample is Iron-di-silicide ($FeSi_2$). The RHEED images before, during and after deposition of Fe are shown in Figure 40, Figure 41 and Figure 42 respectively. The measurements are taken at point A on Figure 40.

---

[*]National Instruments Corporation, http://www.ni.com/legal/termsofuse/unitedstates/us/

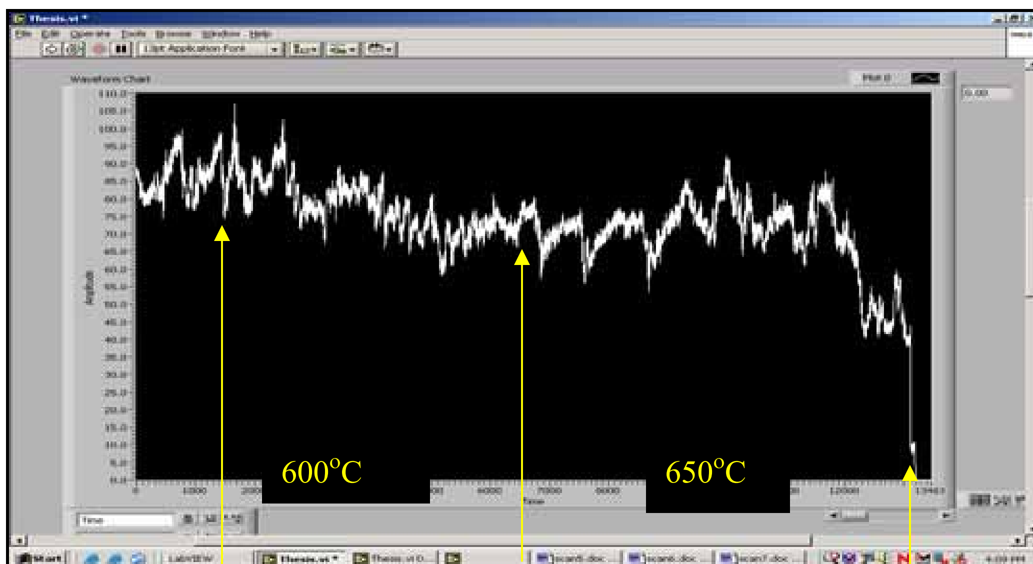

Figure 39. RHEED oscillations for sample-1 and sample-2 recorded using LabVIEW® program.

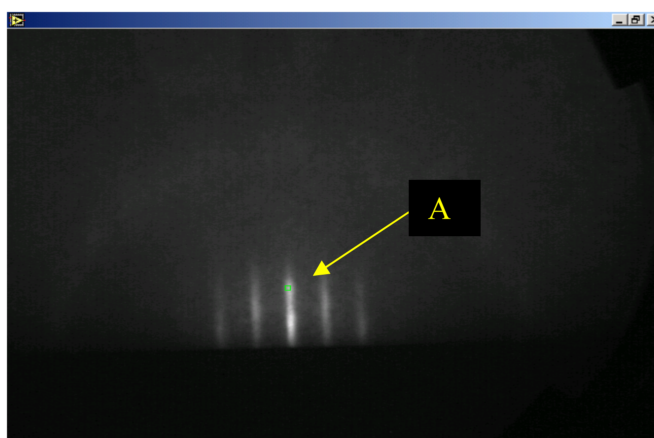

Figure 40. RHEED image before growing Fe for sample-1.

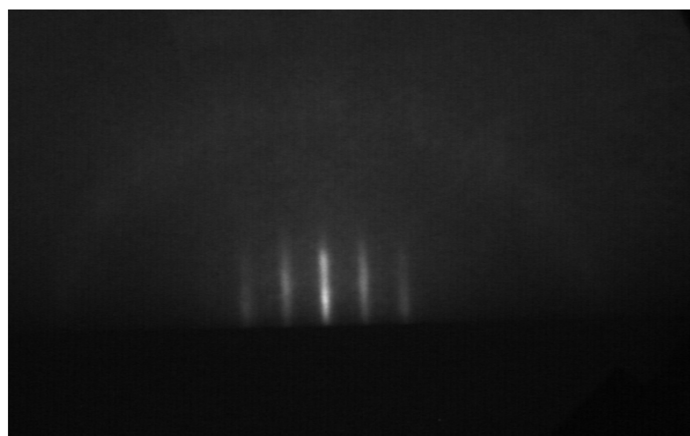
Figure 41. RHEED image for sample-1 during the growth.

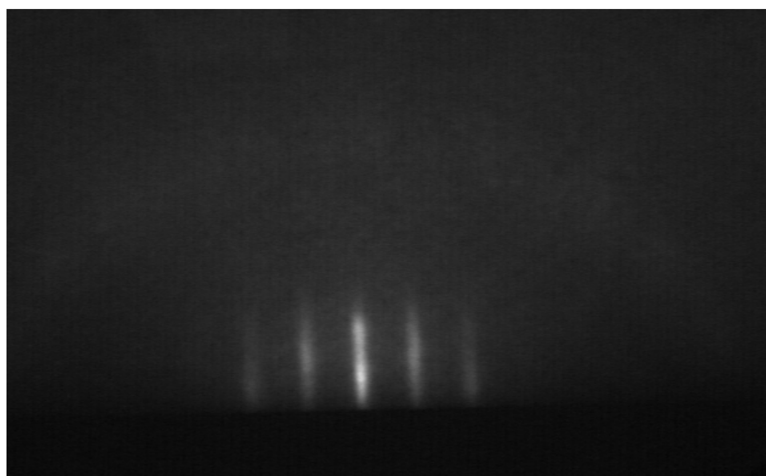

Figure 42. RHEED image for sample-1 after finishing Fe deposition.

Sample data is shown in Table 1. The first table of the column represents the time axis in milliseconds. Here, the time count is maintained by the 'Wait until next ms multiple', LabVIEW® delay timer. The timer stores the latest millisecond value it had counted during the previous run; when called again, it starts the count from this last value. For example, if the first value on x-axis is 11949050, the 50 milliseconds delay will make the second value on the X-Axis as 11949100 (11949050+50=11949100). The second column is the Y-axis represents the output value of the analog-to-digital (ADC) on the frame grabber card in milli volts (mv).

The graph is now reconstructed using the ORIGIN mathematical software, which can calculate the fast Fourier transform (FFT) of a given set of data. ORIGIN first plots the graph on a 2-dimensional X-Y graph. Then with the help of a movable cursor, the starting point and the end points on the graph can be selected; ORIGIN provides the FFT of the selection. For easier interpretation of the graph, the huge millisecond values recorded by the timer are converted to seconds. In order to do this, a new column (column B) is created. The value of column B will be (column (A)-11949000)/1000. The value 11949000 is chosen to get the closest approximate rounded value in seconds. These new values form the X-Axis in the reconstructed graph. The final values are shown in Table 2. Dr. Gossmann's program gives the time value in direct

milliseconds, so for converting the value in seconds, the X-Axis values are divided by 1000. Sample data from Dr.Gossmann's program is shown in Table 3. The reconstructed graph is shown in Figure 43. The data from Dr.Gossmann's program is reconstructed using ORIGIN software and is shown in Figure 44. Data was taken using both the systems for approximately 4.2 minutes.

Table 1. RHEED data from LabVIEW® program.

Time (ms): X-Axis	Amplitude (mv): Y-Axis
11949050	87.889
11949100	86.333
11949150	86.333
11949200	87
11949250	88.889
11949300	86.667
11949350	88.333
11949400	86.222
11949450	87.556
11949500	87.556
11949550	85.889
11949600	86.333
11949650	85.667
11949700	85.778
11949750	87.667
11949800	88
11949850	85.889
11949900	86.333
11949950	85.667
11950000	87.222
11950050	86.889
11950100	88.333
11949050	87.889
11949100	86.333
11949150	86.333
11949200	87
11949250	88.889

Table 2. Reconstruction of RHEED oscillations in ORIGIN program for LabVIEW® for sample-1.

Column A	Column B	
Time (ms) X-axis	Time (s) X-axis	Amplitude (mv) Y-Axis
11949050	0.05	87.889
11949100	0.1	86.333
11949150	0.15	86.333
11949200	0.2	87
11949250	0.25	88.889
11949300	0.3	86.667
11949350	0.35	88.333
11949400	0.4	86.222
11949450	0.45	87.556
11949500	0.5	87.556
11949550	0.55	85.889
11949600	0.6	86.333
11949650	0.65	85.667
11949700	0.7	85.778
11949750	0.75	87.667
11949800	0.8	88
11949850	0.85	85.889
11949900	0.9	86.333
11949950	0.95	85.667
11950000	1	87.222
11950050	1.05	86.889
11950100	1.1	88.333
11950150	1.15	88
11950200	1.2	88.111
11950250	1.25	86.556
11950300	1.3	86.778

Table 3. Reconstruction of RHEED oscillations in ORIGIN for Dr.Gossmann's program for sample-1.

Column A	Column B	
Time (ms) X-Axis	Time (s) X-Axis	Amplitude (μ volts) Y-Axis
77	0.077	98501
144	0.144	98463
210	0.21	97703
277	0.277	97566
344	0.344	97833
411	0.411	97811
477	0.477	96621
678	0.678	96006
747	0.747	96246
844	0.844	96248
911	0.911	95838
978	0.978	97155
1047	1.047	97927
1145	1.145	97093
1264	1.264	97163
1345	1.345	99665
1412	1.412	99705
1478	1.478	99822
1545	1.545	101121
1612	1.612	100586
1679	1.679	100847
1745	1.745	99709
1812	1.812	101175
1879	1.879	103284
1946	1.946	104569

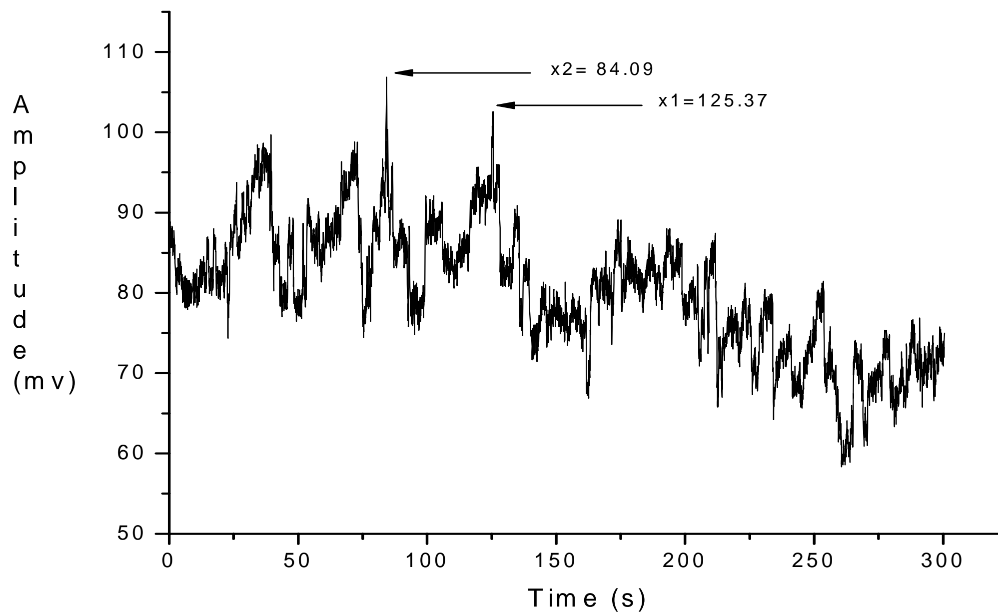

Figure 43. Reconstruction of RHEED oscillations for LabVIEW® using ORIGIN.

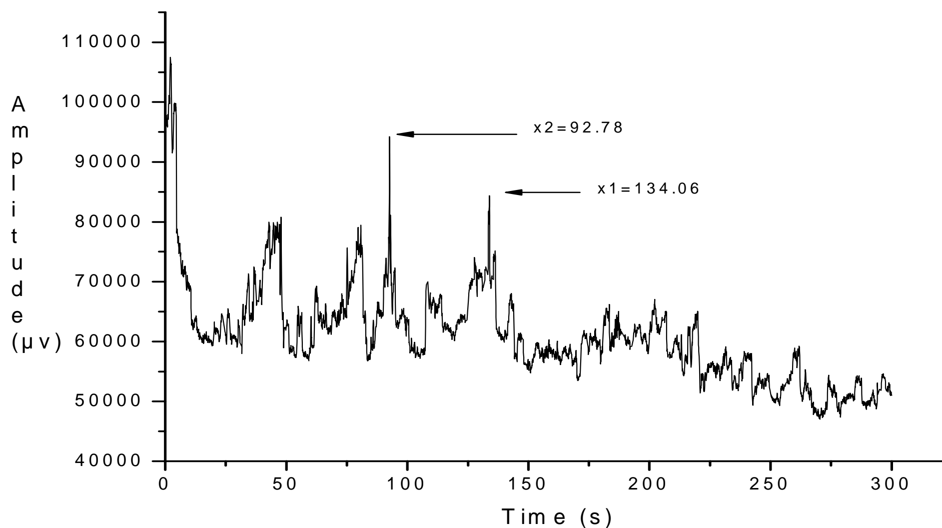

Figure 44. Reconstruction of RHEED oscillations for Dr.Gossmann's program using ORIGIN.

It can be seen from Figure 43 and Figure 44 that the oscillations obtained from two different sources have an identical pattern of growth. Consider two points on time axis for Figure 47, x1=125.37 and x2=84.09, x1-x2=41.28 s. The time difference between two major peaks

obtained using LabVIEW® is 41.28s. Consider the value on X-axis for similar peaks obtained using Dr.Gossmann's program in Figure 45. x1-x2=134.06-92.78= 41.28s. Therefore, the time difference at which the peaks are occurring in the oscillations is equal, even though they are captured using two different programs. Now FFT calculations are made on these graphs to know the growth rates. The FFT for Figure 43 is shown in Figure 45 and the FFT for Figure 44 in shown in Figure 46. A definite peak value can be observed on the FFT graph for LabVIEW® at 0.85 Hz which is the growth rate, and for Dr.Gossmann's program at 0.82 Hz.

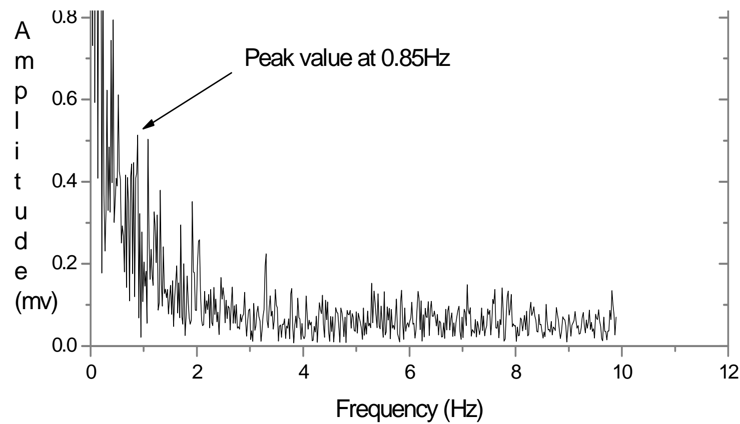

Figure 45. FFT for LabVIEW® for sample - 1.

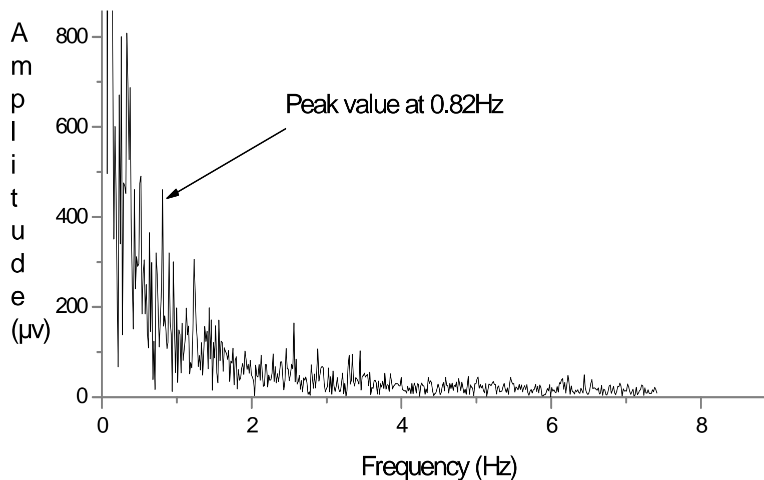

Figure 46. FFT for Dr.Gossmann's program for sample -1.

Now for sample-2, the reconstruction using ORIGIN for both LabVIEW® and Dr.Gossmann's programs are shown in Figures 50 and 51, respectively. The readings were taken for approximately 5.84 minutes using both the programs. Sample data readings for both the software's are shown in Tables 4 and 5. For LabVIEW®, the time in milli seconds into seconds by the formula (Column (A)- 12249500)/1000. For Figure 50 again the difference between two peak points is x1-x2=286.50-201.85=84.65s, for Figure 51 it is again x1-x2=294.77-211.41=83.36s. The RHEED images before, during and after the deposition are shown in Figure 52, Figure 53 and Figure 54 respectively, the measurements are made at point A in Figure 52. It can be observed that the RHEED images in Figures 52, 53 and 54 at 650°C are dull when compared to images in Figures 43, 44, and 45 at 600°C. The FFT calculation for data using LabVIEW® and Dr.Gossmann's program are shown in Figures 55 and 56, respectively. Here, both oscillations yield peak at 1.12Hz, providing an exact 100% match.

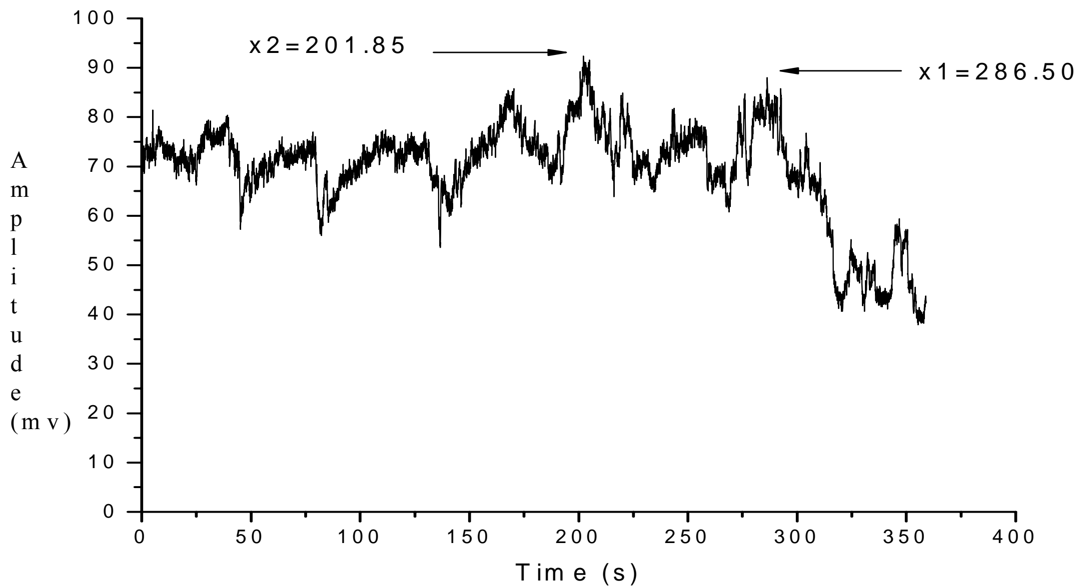

Figure 47. RHEED reconstruction for sample-2 for LabVIEW® program.

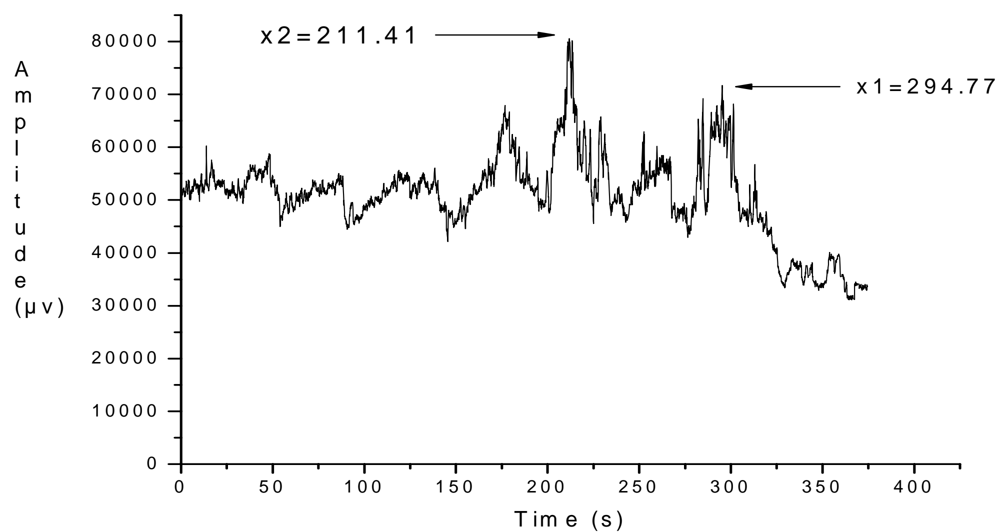

Figure 48. RHEED reconstruction for sample-2 for Dr.Gossmann's program.

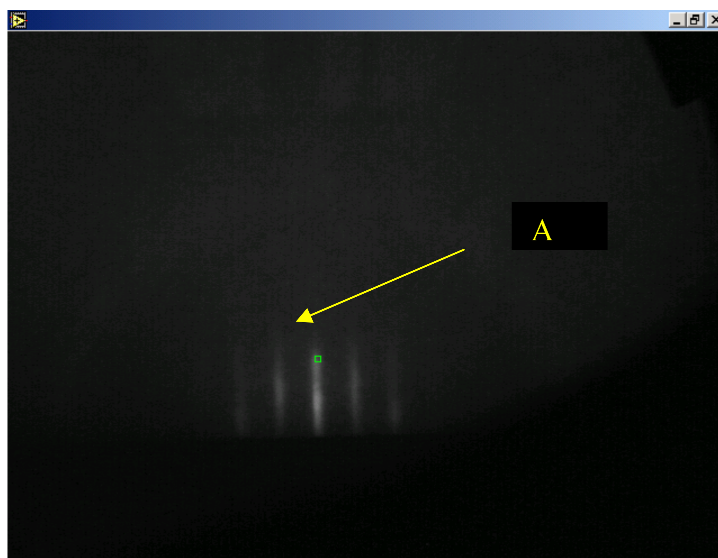

Figure 49. RHEED image before deposition of Fe on sample-2.

Table 4. Reconstruction of RHEED oscillations in ORIGIN program for LabVIEW® for sample - 2.

Column A	Column B	
Time (ms) X-axis	Time (s) X-axis	Amplitude (mv) Y-Axis
12249500	0	72.556
12249550	0.05	73.667
12249600	0.1	72.444
12249650	0.15	72.778
12249700	0.2	72.556
12249750	0.25	73
12249800	0.3	72.889
12249850	0.35	72.889
12249901	0.401	70.111
12249950	0.45	70.778
12250000	0.5	69.889
12250050	0.55	69.556
12250100	0.6	69
12250150	0.65	71.222
12250200	0.7	71.778
12250250	0.75	71.111
12250300	0.8	72.667
12250350	0.85	74.222
12250400	0.9	73.444
12250450	0.95	71.444
12250500	1	71.444
12250550	1.05	70.444
12250600	1.1	69.778
12250650	1.15	69.889
12250700	1.2	68.556
12250750	1.25	69.556
12250800	1.3	72.111

Table 5. Reconstruction of RHEED oscillations in ORIGIN for Dr.Gossmann's program for sample-2.

Column A	Column B	
Time (ms) X-Axis	Time (s) X-Axis	Amplitude (μv) Y-Axis
300086	0.086	50980
300153	0.153	49911
300220	0.22	49774
300286	0.286	49985
300353	0.353	50004
300420	0.42	50445
300487	0.487	50903
300553	0.553	51387
300620	0.62	51350
300687	0.687	51245
300754	0.754	50919
300820	0.82	51058
300887	0.887	51238
300954	0.954	51344
301020	1.02	51532
301087	1.087	51669
301162	1.162	52101
301254	1.254	51532
301321	1.321	51993
301388	1.388	52307
301454	1.454	52127
301521	1.521	51679
301588	1.588	51799
301655	1.655	51456
301721	1.721	51759

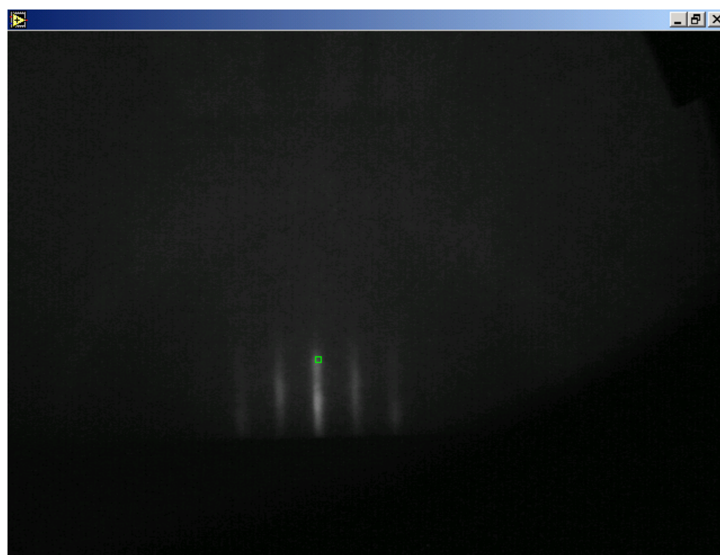

Figure 50. RHEED image during deposition of Fe on sample-2.

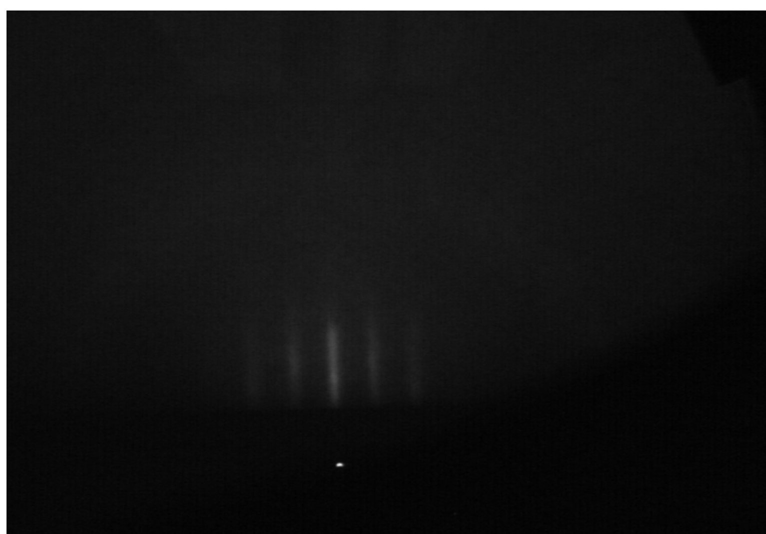

Figure 51. RHEED image after depositing of Fe on sample-2.

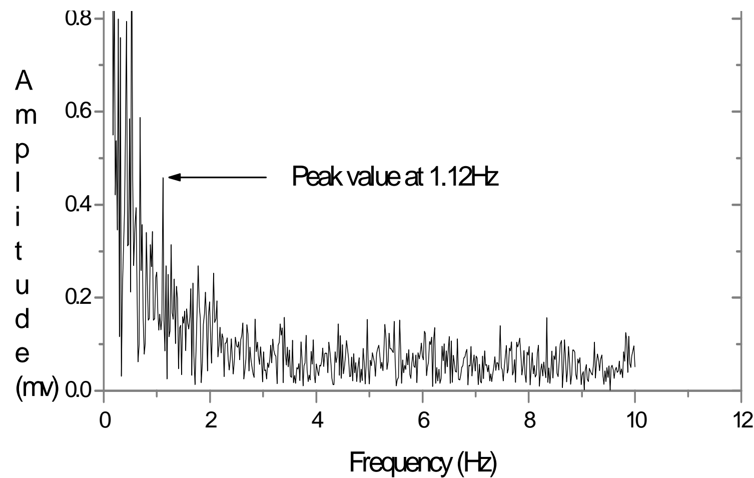

Figure 52. FFT for LabVIEW® program for sample-2.

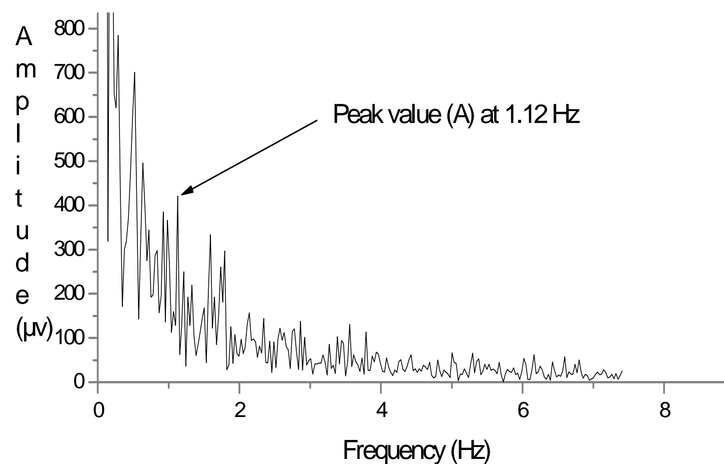

Figure 53. FFT for Dr.Gossmann's program for sample - 2.

Now that the acquisition of RHEED oscillations and calculation of FFT has been demonstrated successfully, the importance of capturing RHEED images will be concentrated on next sample. This sample will be called sample-3. Using the LabVIEW® program the user also has flexibility to change the point at which the intensity measurements are made on the RHEED image. This provides flexibility to observe the growth rate at different points on the crystal, giving a better idea on how the crystal is being formed on different areas of a substrate. This time

a layer of Si was grown on a Si wafer for 10 minutes at 500˚C. Then a layer of Fe is grown for 19 minutes at 550˚C. Next a layer of Ge is grown for 4.5 minutes at 475˚C. The oscillations captured during the growth are shown in Figure 54.

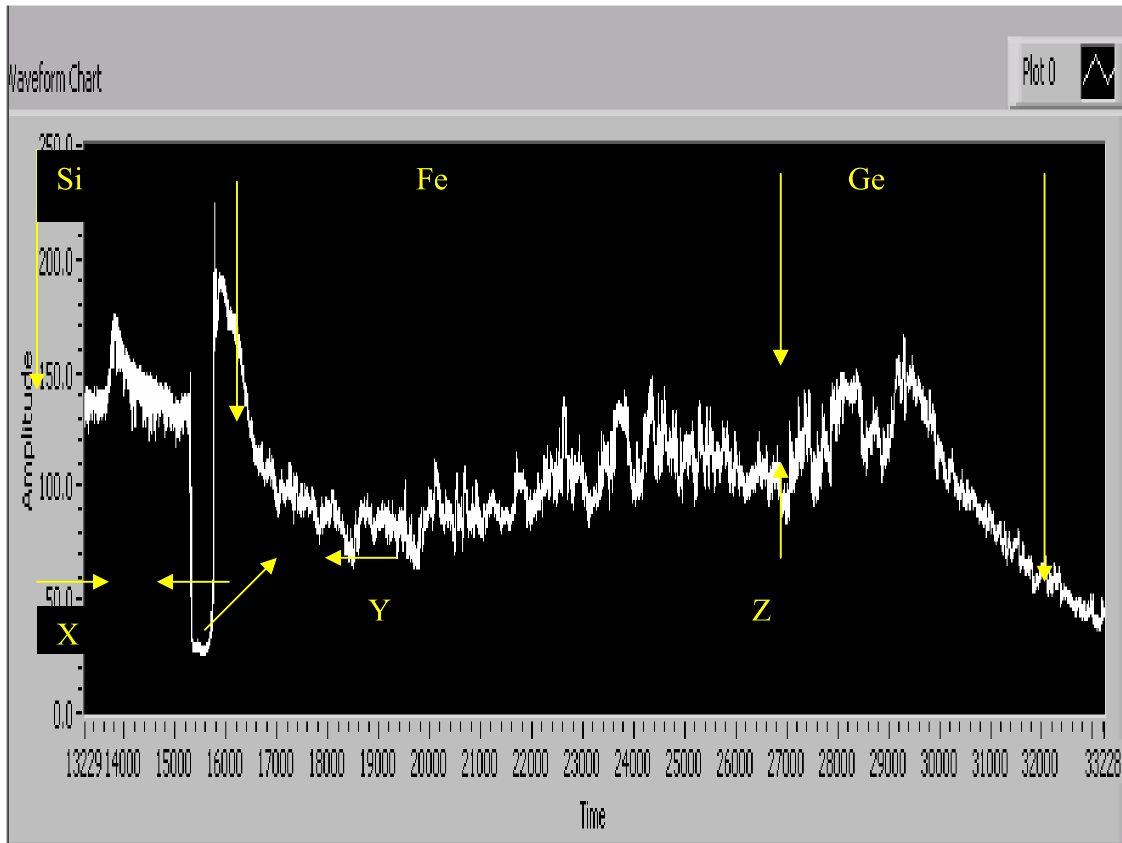

Figure 54. RHEED intensity recording for sample-3.

The RHEED images recorded during the various stages of growth are shown in Figure 55 through Figure 61. The RHEED oscillations are recorded at point A shown in Figure 55. Approximately after 411 seconds the RHEED image moves from its position. So the point at which the measurement is made completely dark, so to record the right oscillations the point of measurement is changed using the 'Coordinate System' control present on the front panel. The current X and Y co-ordinates on the chart where the measurement is being made are entered in the 'Reference System'. The final co-ordinates where the point of measurement has to be shifted

is entered in the ‘Measurement System’. The measurement point then automatically shifts by the difference between the Reference System and Measurement System. The change in the point of intensity of oscillations, which the point of measurement is changed, is observed at point X in Figure 58. During the change in the point of measurement, there is a delay of few milli seconds in the program. The change on the RHEED image is observed in Figure 54. When the Fe source is opened, the RHEED image changes instantaneously from Figure 56 and Figure 57. After 413 seconds the RHEED image shifts again, so the point of measurement is shifted accordingly. This is shown as point Y in Figure 54. The change in the point of measurement can be seen on RHEED image in Figure 56. When the Ge source is opened the RHEED image changes from Figure 58 to Figure 59. The intensity of the oscillations also decreases and this can be observed at point Z in Figure 54. At the end of deposition of Ge the RHEED image becomes almost invisible as shown in Figure 61. From Figure 55 through Figure 61 it can be observed that the RHEED images are different for different materials even though they are being grown as a single sample.

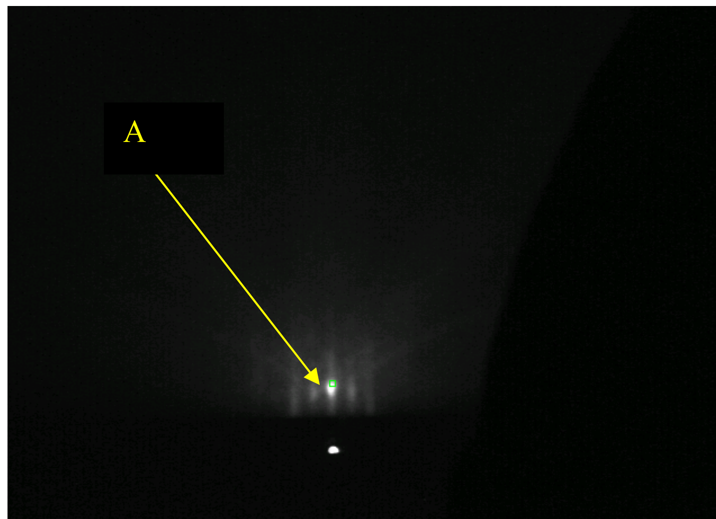

Figure 55. RHEED image during initial deposition of Si.

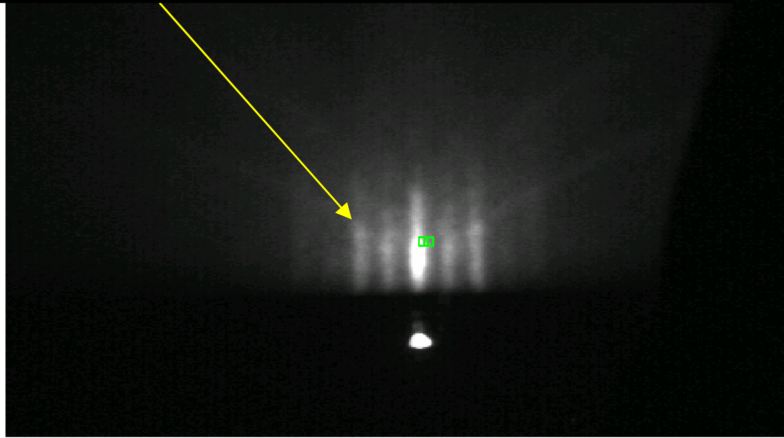

Figure 56. RHEED image after depositing Si for 8 minutes.

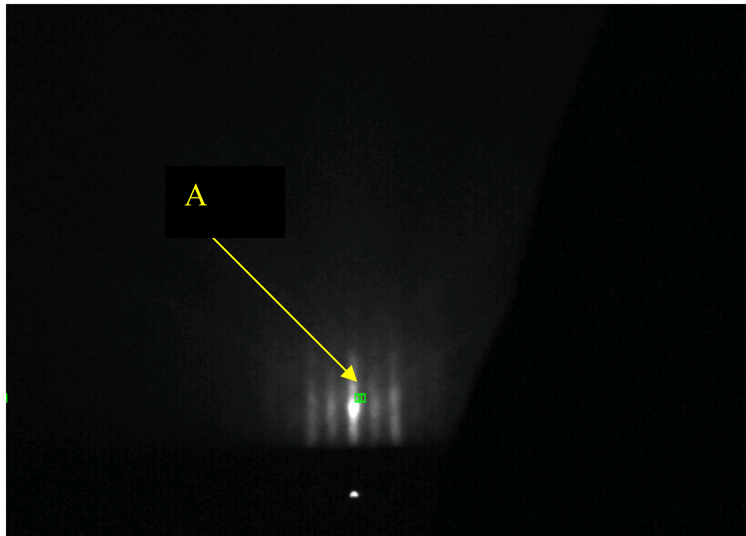

Figure 57. RHEED image when the Fe source is opened.

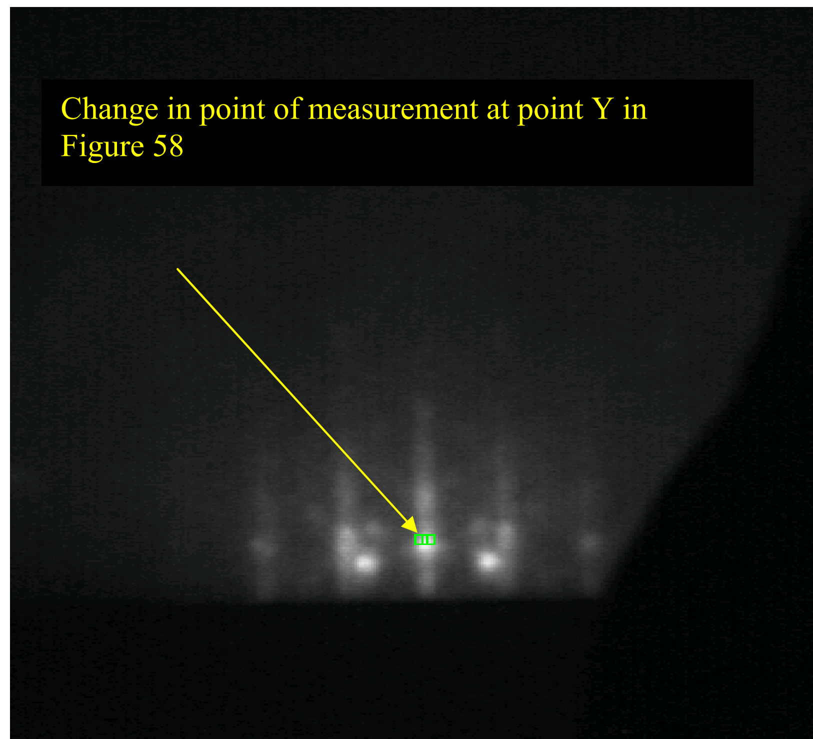

Figure 58. RHEED image after depositing Fe for 15 minutes.

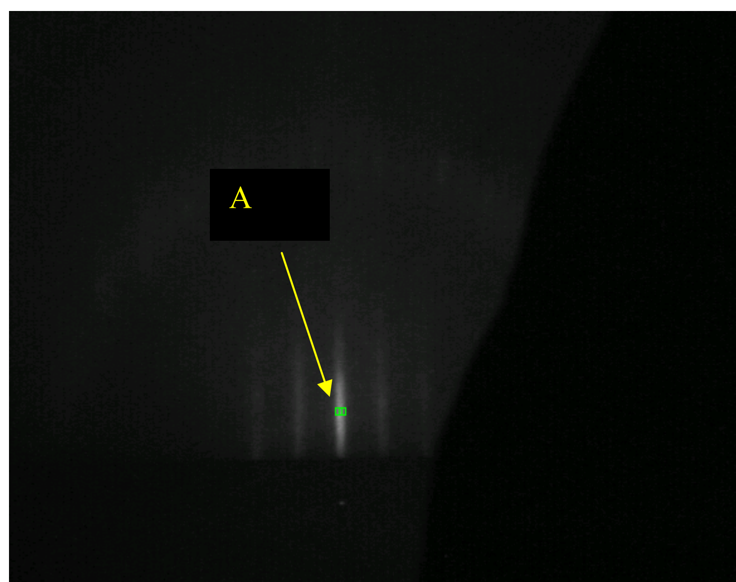

Figure 59. RHEED image after Ge source is opened.

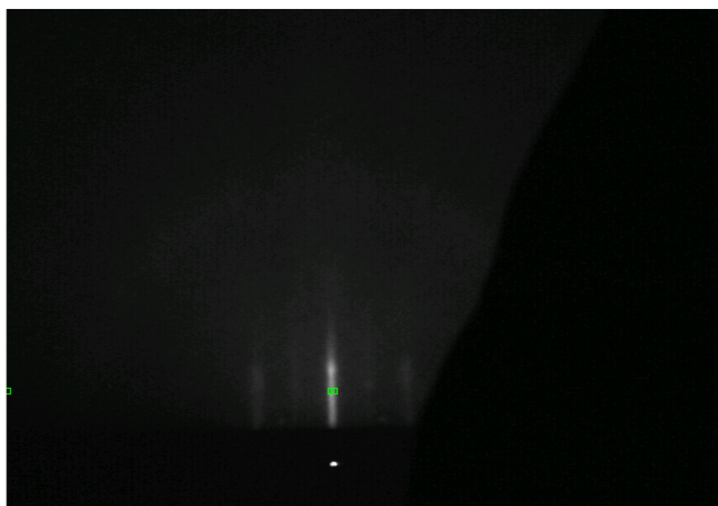

Figure 60. RHEED image after depositing Ge for 2 minutes.

Figure 61. RHEED image at the end of depositing Ge.

The growth pattern is reconstructed using ORIGIN software and is shown in Figure 62. The oscillations observed while depositing Si, Fe and Ge are shown here are similar to Figure 54. When the reference point is being changed there is a small delay introduced in the program. The

reference point was changed twice while taking the readings for this growth and can be observed at points X and Y in Figure 62. The FFT calculations at various stages of growth are shown below. Figure 63 shows the growth pattern when Si is being deposited. The FFT has a predominant peak at approximately 1.8Hz. Figure 64 shows the growth pattern when Fe is being deposited. The FFT has a predominant peak at approximately 1.6Hz. Figure 65 shows the growth pattern when Ge is being deposited. The FFT has a peak at approximately 1.9 Hz.

From the FFT calculations it can be observed that different materials exhibit different RHEED patterns and exhibit different RHEED patterns. These RHEED oscillations and images can be saved and can be compared with the data obtained from the similar samples that are being grown. These samples are then sent out for further analysis to test if they exhibit required characteristics. Once the good samples are identified, the related RHEED data can be pulled out and be used to grow similar wafers on a large scale production basis.

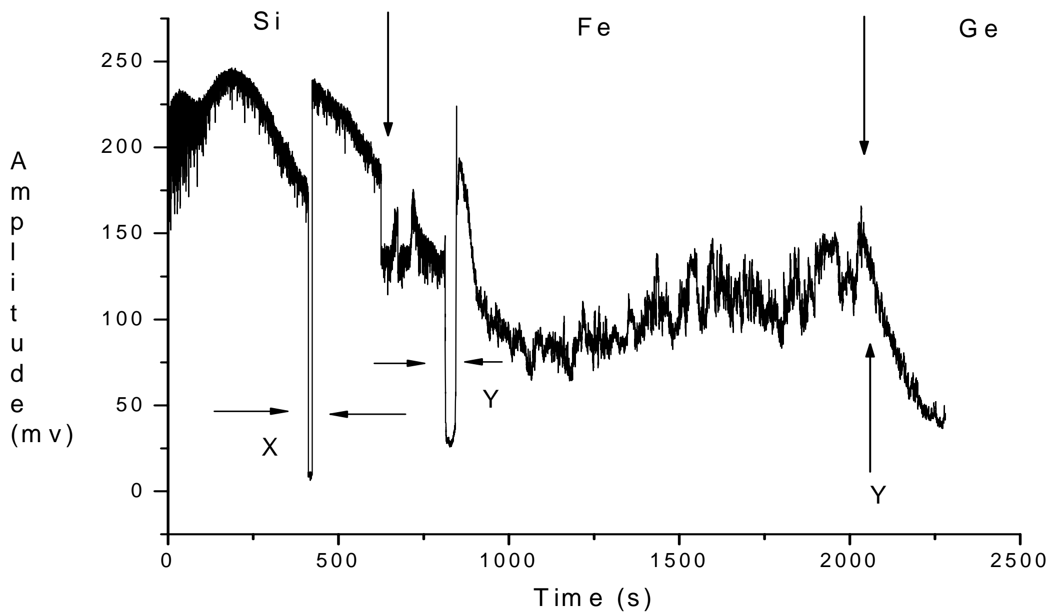

Figure 62. Growth pattern reconstructed using ORIGIN software.

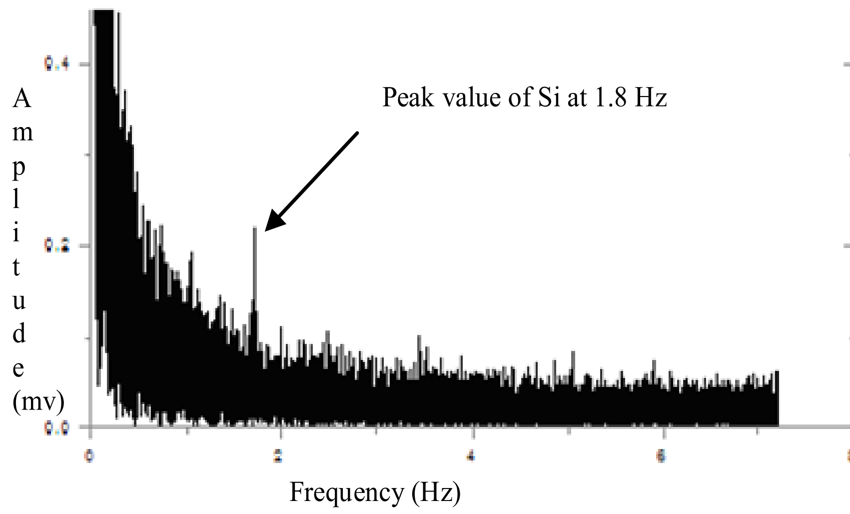

Figure 63. FFT of oscillations for Si growth.

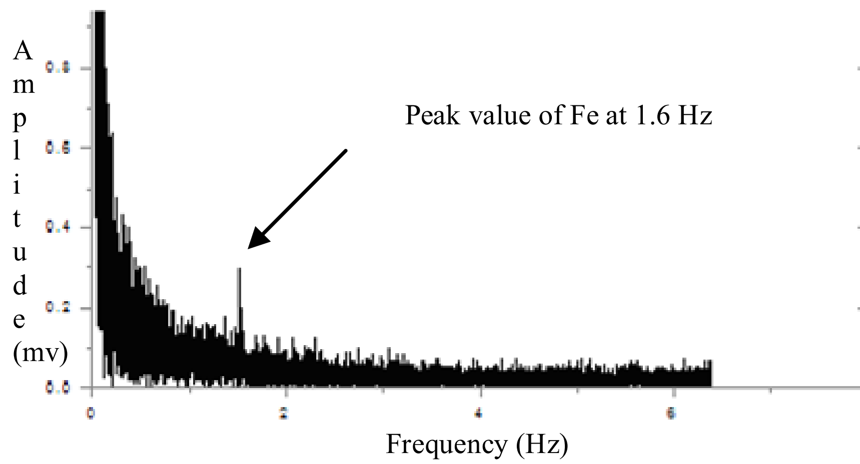

Figure 64. FFT oscillations for Fe Growth.

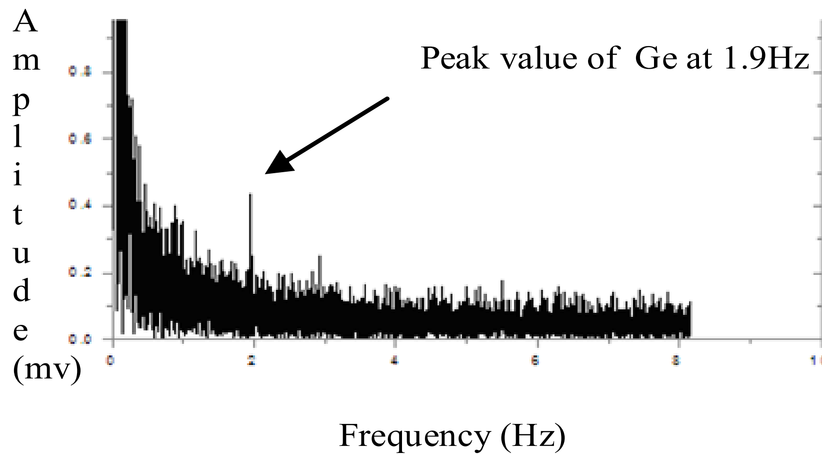

Figure 65. FFT oscillations for Ge

Limitations

This program is limited to be used with NI-IMAQ 1409 frame grabber card. The data acquisition rate of the frame grabber card is limited to 30 frames/second with an NTSC camera, 25 frames/second with a PAL camera and 60 frames/second with a progressive scan camera. For this program a NTSC camera is used. The program works with the LabVIEW® version 6.1 or higher. It is also necessary to have the complete NI-IMAQ VISION library accompanying the LabVIEW® 6.1 full development system, for proper functioning of NI-IMAQ sub VIs. The accuracy of the intensity of oscillations being captured depends highly on the resolution of the camera. In this program the intensity is recorded every 50 milli seconds.

CHAPTER V

CONCLUSIONS

The video reflection high-energy electron diffraction (RHEED) intensity measurement program which was used previously on the III/V molecular beam epitaxy (MBE) system did not have a provision to store the RHEED images. The fast Fourier transform (FFT) calculations made on the recorded intensity graphs could not be saved too. These limitations have been overcome using this Lab VIEW program[*]. The LabVIEW® code can record the RHEED intensity oscillations, RHEED images, save the data to an EXCEL sheet. With the help of ORIGIN software FFT calculations can be made successfully on the data obtained from the LabVIEW® code. The RHEED images can be recorded at any particular point of time during the growth and the FFT calculations can be stored effectively. Also the Video RHEED program made use of an extra monitor to observe the oscillations in addition to the use of a computer to view the RHEED images. Using LabVIEW® code the intensity of the oscillations can be recorded using the same computer on which the RHEED images are being observed.

Also, the Video RHEED program did not have a facility to record the intensity values to a text file or an EXCEL sheet, it was only in the form of a graph, the individual data values could not be stored on a different file. So if the data needs to be transported to any other program for analysis it could not be done so. Using the LabVIEW® program the data can be stored in a text file or an EXCEL sheet for future analysis. Also during crystal growth, the RHEED patterns change continuously. This results in the shift of the image. So during the growth process the point at which the measurement is taken needs to be shifted also to get accurate readings. The LabVIEW® program provides a facility to shift the point at which the measurement is being made during the crystal growth providing accurate data for FFT analysis. Also, if more than one

[*] National Instruments Corporation, http://www.ni.com/legal/termsofuse/unitedstates/us/

sample of same kind is being grown on the same day, the oscillations can be appended to the same file if needed. This is particularly useful for comparison purposes when it is need to observe the growth pattern of a single sample under different growth conditions such as temperature and pressure. In the Video RHEED program, if the recording of the oscillations was stopped at a point of time, every time a new file was needed to be opened to record the oscillations. Thus, one or more sets of data could not be appended to the same graph for comparison studies. This limitation has been overcome in the LabVIEW® code.

It can be seen from Figure 39, Figure 47 and Figure 54 that different materials exhibit different RHEED patterns and images depending on their composition and the acquisition of the RHEED patterns becomes more and more difficult as the complexity of the semiconductor material increases. As the RHEED patterns become more complex it becomes even more difficult to calculate their FFTs.

In addition to working on the LabVIEW® code this thesis has also provided an opportunity to learn MBE growth process, MBE source maintanenance, sample preparation, operating the various software's associated with an MBE system and maintaining Ultra High Vacuum conditions for the MBE growth. In the real world semiconductor and electronic industries use LabVIEW® for a number of applications such as Samsung uses NI LabVIEW® and Modular Instruments to Reduce Development Time on Signal Generator Project [24], Toshiba uses PCB Tester system interfaced using LabVIEW®, Lawrence Livermore National Labs uses LabVIEW® for Fabrication Process of Next Generation Microprocessors, G Systems, Inc. designs Flexible Semiconductor Test Executive with LabVIEW® and NI Test Stand, Virginia Semiconductor Incorporation uses automated silicon wafer measurement using NI-IMAQ and LabVIEW®, Texas instrument's characterization process was streamlined with test

development, management, and automation software powered by National Instruments LabVIEW® and NI Test Stand and so on. Working on the MBE system with the help of LabVIEW® software has trained me for practical industrial applications. Therefore, a working LabVIEW® program has been created as an alternative to the Video RHEED Intensity Measurement Program, to monitor the growth of semiconductor materials grown in the III/V MBE system.

CHAPTER VI

FUTURE WORK

An molecular beam epitaxy (MBE) system coupled with a feedback control system can refine the MBE system into a turnkey manufacturing process. A real time MBE control system has to be designed in such a way that it works with the already existing MBE growth systems. It must be able to provide real-time information of the wafer growth states, simple to install and maintain, allow fast processing of data at a low cost.

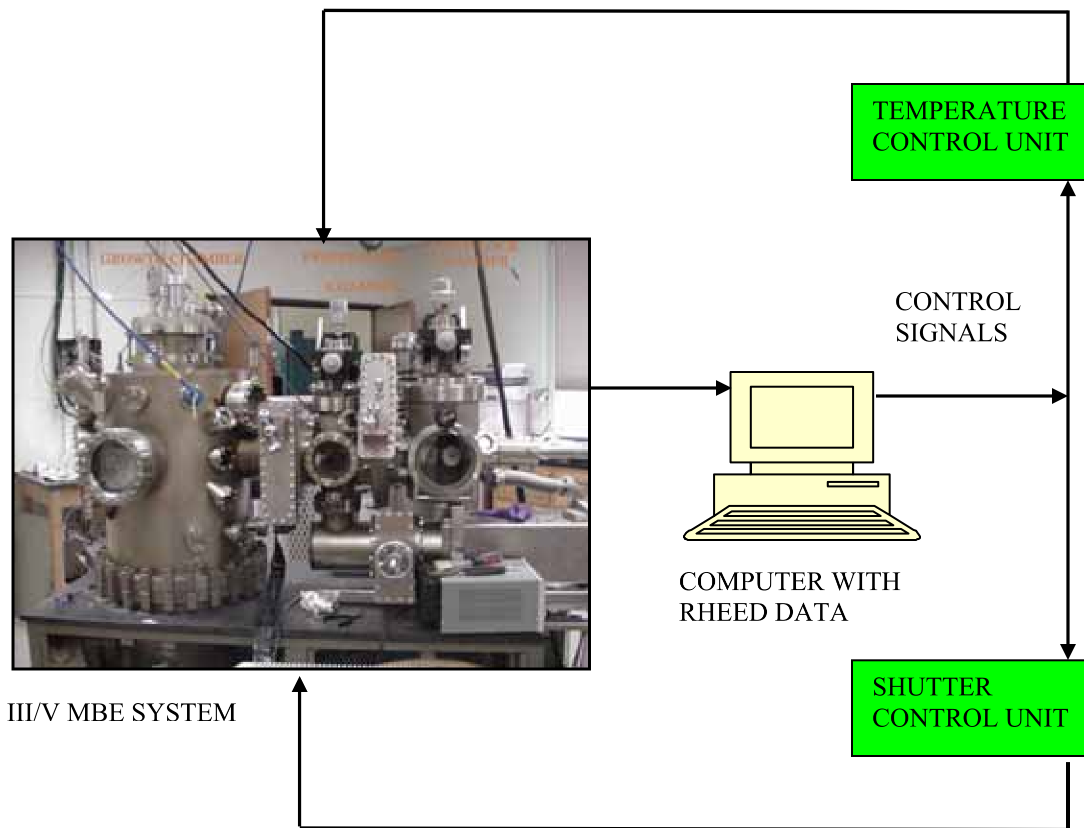

Figure 66. MBE system with a feedback control system associated with it.

The LabVIEW® program[*] discussed above is the first step towards converting MBE to a true mass production technology, shown in Figure 66. The PCI-1409 frame-grabber card used here has four external I/O lines which can be configured as triggers or digital I/O lines. A set of wafers of a particular material can be grown and the real-time reflection high-energy electron diffraction (RHEED) data can be obtained using this LabVIEW® program. The samples are then analyzed to see if they exhibit the desired characteristics. Once the working samples are identified the defective samples can be eliminated and also the RHEED data associated with it. The working samples data can be stored for further growth process. Another LabVIEW® program can then be written that displays the RHEED images and patterns continuously, when similar wafers are being grown on a large-scale. If the patterns do not match the temperature of the source cells can be altered or the movement of the shutters can be controlled by sending control signals. A control-system has to be designed, that accepts the signals from the computer having the RHEED program and accordingly sends signals to the temperature-control unit and the shutter-control units on the MBE system shown in Figure 66.

Having a before-hand knowledge of the wafers being grown results in dedicated calibration times/runs, early warning of out-of-spec growth, increase in run-to-run production, provides growth information of wafers for customers process correlation and feedback. A closed-loop MBE will thus pave the way for a truly production MBE system thereby increasing yield and decreasing the cost of production.

[*] National Instruments Corporation, http://www.ni.com/legal/termsofuse/unitedstates/us/

REFERENCES

1. T.Mimura, S.Hiyamizu, T.Fujii and K.Nanbu, A new FET with selectively doped GaAs/n-$Al_xGa_{1-x}As$ Heterojunctions, J.Appl.Phy. 1a,L225(1980).

2. A.Gruble, H.Kibbel, U.Erben and E.Kasper, MBE grown HBTs with High β, f_{To} and f_{max} , IEEE Electron Device Lett., 13,206 (1992).

3. A.Y.Cho and D. R, Ch'en, GaAs MESFET prepared by Molecular Beam Epitaxy, Applied Physics Letters, 28, 30(1976).

4. A.Y.Cho and K.Y.Cheng, Growth of extremely uniform layers by rotating substrate holder with MBE for applications to electro-optic and microwave devices, Appl. Phys. Lett. 38, 360 (1981).

5. E.Kasperand K.Worner, High Speed Integrated Circuits using Si MBE, J.Electrochem, Soc., solid-state science and Technology, 2481(1985).

6. M.A.Hoase, J.Qui, J.M.DePuydt, H.Cheng, Blue-Green laser diodes, Appl.Phys.Lett.59, 1272(1991).

7. H.Temkin, T.P.Pearsall, J.C.Bean, R.A.Logan and S.Luryi, Ge_xSi_{1-x} strained-layer supperlattice waveguide photodetectors operating near 1.3μm.

8. Eason, D.B. Yu, Z. Hughes, W.C. Bon, C. Cook, J.W. Schetzina, J.F. He, Y.W. Masry, N.A.E. Cantwell, G. Harsch, W.C, High-Brightness Blue & Green LEDs Grown by MBE on ZnSe Substrates.

9. S.Shah, T.J.Garrett et all., Pattern based investigation of the length-scale dependence of the surface evolution during multilayer epitaxial growth, Appl.Phys.Lett.83, 4330 (2003).

10. RF micro devices 6in GaAs wafer fabrication, Greensboro, NC, USA. http://www.semiconductor-technology.com/projects/rf , 12/15/2003.

11. Davey, J.E. Pankey, T. 1968. J. Appl. Phys, 39: 1941-48.

12. J.S.Resh, K.D.Jamison, J.Stozier, and A.Ignatiev, Multiple reflection high-energy electron diffraction beam intensity measurement system. Space Vacuum Epitaxy Center, University of Houston, Houston, Texas, 77204-5507.

13. Video RHEED Intensity Measurement System, Program: RHEED manual, Epitaxial Growth Systems, Houston, TX.

14. Gunther, K.G. 1958. Z. Naturforsch. Teil A 13:1801-89.

15. W.Braun. Applied RHEED. Reflection High-energy Electron Diffraction during Crystal Growth. 1999. Springer Tracts in Modern Physics, 154. 2.

16. Harris Benson, University Physics.

17. Solid State Physics, Charles Kittel, Wiley Publications, 7th Edition,1995.

18. MBE Varian 360 manual, Operations and Routine Maintenance, Varian Industrial Equipment Group,1978.

19. Klaus Ploog. Ann. Rev. Material Sci. 1981. 11-171-210, Molecular Beam Epitaxy of III-V Compounds: Technology and Growth Process.

20. Spec View Plus software – User Guide, Spec View LLC, February 1, 2000.

21. National Instruments, NI PXI – 1409, http://www.ni.com/pdf/products/us/3vis591-593.pdf , 01/06/2003.

22. Robert H.Bishop, Learning with LabVIEW® 6.i.

23. IMAQ VISION for LabVIEW® user manual, http://www.ni.com/pdf/manuals/371007a.pdf, 08/01/2003.

24. Customer solutions in semiconductor industry, http://sine.ni.com/csol/cds/list/vw/p/qry/ind/id/Semiconductor/srt/dt_d/nid/124200